Neutrophil Extracellular Trap Mediated Radio-Resistance in Early-Stage Non-Small Cell Lung Cancer

Malcolm I. Ryan

MSc. Thesis

Table of Contents

Article I. Abstract

Introduction: Non-small cell lung cancer (NSCLC) remains a leading cause of cancer-related deaths, even when diagnosed in its early stages. Currently, the standard treatments are surgery and stereotactic ablative radiotherapy (SABR). Despite these interventions, a significant number of patients will experience locoregional recurrence after undergoing SABR, particularly when dealing with larger tumors. Recent research has brought attention to the role of Neutrophil Extracellular Traps (NETs), which are released from neutrophils during inflammatory reactions. Here we aim to investigate whether NETs play a role in radio-resistance in NSCLC and to understand the underlying mechanisms driving resistance.

Methods: To explore the role of NETS in radio-resistance, we used an orthotopic model of NSCLC where LLC1 cancer cells were injected into the left lung of wildtype or NET deficient *Pad4-/-* mice. Mice were then irradiated 7 days after tumor implantation. Tumor kinetics were measured over time and the tumor microenvironment was characterized with spectral flow cytometry and immunofluorescence spectroscopy. Further, we also tested the effect of NETs in the context of combination radiotherapy (RT) + immunotherapy. In parallel, we collected NSCLC samples for imaging mass cytometry (IMC) from 3 cohorts of patients that either received neoadjuvant radiation before surgery during the SARs-CoV-2 pandemic, combination chemotherapy radiation, or were treatment naïve, to explore the dynamics of radio resistance in the human tumor microenvironment (TME).

Results: Irradiated *Pad4-/-* mice had significant decrease in both tumor volume and burden in comparison to controls. Further, PD1+ CD8+ T cell infiltration in irradiated *Pad4-/-* mice was significantly increased in comparison to controls. Survival analyses demonstrated that irradiated *Pad4-/-* mice that received adjuvant immunotherapy treatment had significantly better OS in

comparison to wildtype controls. Analysis of the IMC data will be performed in the future to corroborate preclinical results.

Conclusions: NETs play a role in radio resistance through decreasing T cell infiltration in a NSCLC orthotopic setting. Further, in *Pad4-/-* preclinical models, adjuvant immunotherapy was more effective in conferring greater OS. This highlights the potential of a NET-directed therapy to increase SABR induced T cell infiltration in the context of adjuvant immune checkpoint-inhibitor therapy (ICI), improving the early-stage outcomes in a disease where later stages have far poorer mortality.

Article II. Resume

Introduction: Le cancer du poumon à cellules non-petites (CPCNP) reste l'une des principales causes de décès liés au cancer, même lorsqu'il est diagnostiqué à ses débuts. Actuellement, les traitements standards sont la chirurgie et la radiothérapie stéréotaxique ablative (SABR). Malgré ces interventions, un nombre important de patients connaîtront une récidive locorégionale après avoir subi de la radiothérapie, en particulier lorsqu'il s'agit de tumeurs plus volumineuses. De récentes recherches ont attiré l'attention sur le rôle des pièges extracellulaires de neutrophiles (NET), qui sont libérés par les neutrophiles lors de réactions inflammatoires. Nous visons ici à déterminer si les NET jouent un rôle dans la radio-résistance dans le CPCNP et à comprendre les mécanismes sous-jacents à l'origine de la résistance.

Méthodes : Pour explorer le rôle des NET dans la radiorésistance, nous avons utilisé un modèle orthotopique de CPCNP dans lequel des cellules cancéreuses LLC1 ont été injectées dans le poumon gauche de souris Pad4$^{-/-}$, déficients en NET, ou de souris contrôles. Les souris ont ensuite été irradiées 7 jours après l'implantation des tumeur. La cinétique de croissance des tumeurs a été mesurée au fil du temps et le microenvironnement tumoral a été caractérisé par cytométrie spectrale en flux et spectroscopie d'immunofluorescence. De plus, nous avons également testé l'effet des NET dans le contexte d'une combinaison radiothérapie (RT) + immunothérapie. En parallèle, nous avons collecté des échantillons de CPCNP pour la cytométrie de masse par imagerie (IMC) auprès de 3 cohortes de patients ayant reçu une radiothérapie néoadjuvante, soit avant la chirurgie pendant la pandémie de SRAS-CoV-2, une radiothérapie de chimiothérapie combinée ou naïfs de traitement, pour explorer la dynamique de larésistance à la radiothérapie dans le microenvironnement tumoral humain (TME).

Résultats : Les souris Pad4$^{-/-}$ irradiées présentaient une diminution significative du volume et de la charge tumorale par rapport aux contrôles. De plus, l'infiltration de lymphocytes T PD1+ CD8+ chez les souris Pad4$^{-/-}$ irradiées était significativement augmentée par rapport aux contrôles. Les analyses de survie ont démontré que les souris Pad4$^{-/-}$ irradiées ayant reçu un traitement d'immunothérapie adjuvante présentaient une survie globale significativement meilleure par rapport aux contrôles. L'analyse des données IMC sera effectuée à l'avenir pour corroborer les résultats précliniques.

Conclusions: Les NET jouent un rôle dans la radiorésistance en diminuant l'infiltration des lymphocytes T dans un contexte orthotopique de CPCNP. De plus, dans les modèles précliniques Pad4$^{-/-}$, l'immunothérapie adjuvante était plus efficace pour conférer une meilleure survie globales. Cela met en évidence le potentiel d'une thérapie dirigée vers les NET pour augmenter l'infiltration de lymphocytes T réduites par la radiothérapie. Ceci pourrait avoir comme effet d'augmenter la réponse aux inhibiteur de point de contrôle immunitaire, améliorant ainsi les chances de survies des patients attients d'un cancer à un stade précoce.

Article III. Acknowledgments

I would first like to thank my two supervisors, Dr. Logan Walsh, and Dr. Jonathan Spicer for immeasurable mentorship and guidance throughout this project. Logan, you have often helped me zoom out and see the bigger picture in a field where too often we are hyper focused on small details. Jon, your ability to have insight on what seems like a million unrelated topics and still find a way to meaningfully integrate them, will always leave me in awe. Over the past three years you have both helped me hone my interdisciplinary skillset and wherever I end up in the future, I know I owe you both a great deal. Thank you.

It wouldn't be telling the truth to say that I have only two supervisors because of the work of Dr. Roni Rayes. Roni, you have been a steadfast support system, role model scientist, and friend, that when I started my masters got me on the ground running where I probably would've tripped. I want to take this opportunity to thank you for all your help with my radiation trials, last-minute equipment bookings, and printer runs when you were already juggling everything else on your plate. You are very much the glue that holds our lab together and I am grateful to have been a part of it.

I would like to thank France Bourdeau and Valerie Breton for helping me circumvent my poor planning skills, through tireless hours assisting with mouse trials, data analysis, and most importantly making sure I cleaned up after myself. I don't have enough time to list the variety of skills I have picked from your respective brains, but who I am as a scientist is a result of your generous work and time.

I would like to thank Meghan de Meo, the epicenter of the Spicer lab family, for always taking the time to answer questions and make me feel welcome, even when I was running between both my labs like a headless chicken trying to get my flow cytometry to work.

I would like to thank Simon Milette, who much of this thesis is built on the back of. Simon, over the past three years you have gone from an unlikely teacher to irreplaceable friend who I will probably end up alongside backpacking through another small town across the globe. Unfortunately, there is a page count for this thesis, or I would list all your contributions to this project, but please know, I value all the time and support you have given me.

Mark Sorin. As much as that is all I want to type simply because I know we would get a laugh out of it, I must thank you for making up an integral part of the support system I have had for the past three years. Just like you will always admire my basketball and tennis skills, I admire you as a scientist and you inspire me to pursue my goals whatever they may be. Thank you Mark for all your help.

I now need to thank the human encyclopedia, Samuel Dore. Sam, even that characterization does not do you justice. Over the past three years while there have been many ups and downs, the one constant is how amazed I am at your capacity for knowledge, and willingness to help me with anything. I know that I speak for both the Walsh and Quail labs when I say you are an indispensable part of the family that we value immensely. When I'm gone, please remember to reorder the antibodies for OUR flow panel, it is important to stay on top of these things.

I would like to thank Miranda Yu, who contested whether she deserved more than a line in these acknowledgments, when little does she realize I could write a book on all her

contributions to my master's experience. Miranda thank you for keeping me grounded, being a leader, and providing an ear to listen to the laundry list of problems I encountered, even while you had a mountain of your own to climb. I value our friendship and I am excited to see you take the scientific world by storm.

3234$. Lysanne Desharnais, that amount seems well worth it for the friendship we have built over the past 3 years. I want to thank you for providing a sense of normalcy in an environment that can be pretty terrifying at times. You have always been someone who I can relate to and is open to listening, which I learned was sometimes all I really needed. Although please note that next time, I will be taking the window seat.

I would like to thank my research advisory committee for guiding me through this thesis and providing the support and resources to accomplish various aspects of this project. Additionally, I would like to thank all research cores and faculty that assisted me throughout this project.

I would now like to take this time to thank the rest of the Walsh, Spicer, and Quail labs. It almost seems like a dream looking back at how small we were in 2021, to the size we have grown. But just like there appears to be a million new faces, you have all helped me in a million unique ways and for that words are not enough to confer my gratitude. The scientists that graduate from this lab are built on the backs of the *Qualsher* team and thinking back to when I was deciding where to do my masters, I know I made the correct choice.

Andrew Munley, it seems like only yesterday that we were looking for new roommates and you came walking in with that British-Jersey accent of yours that left our brains hurting. Thank you for dealing with my rants, "brilliant" ideas, and everything in between. I know that I

have probably ruined our collective sleep schedules writing this thesis over the past couple months, but who needs a functioning circadian rhythm anyways. This work could not have been accomplished without your support and patience.

I would like to thank my mom for being the spark, the fuel, and the fire that has got me to where I am today. I wouldn't be in the oncology field without the groundwork you laid out and the opportunities that you fought to provide for me. Starting this master's, one of the most exciting aspects was knowing that we would both graduate at the same time and I am so grateful that you are able to pursue your own passions as I bear the fruit of the opportunities you afforded me.

I would like to thank you to my dad for being the steady shoulder to lean on during this experience, always grounding me when the world seemed very much off kilter. I have tried my best to emulate the qualities I admire about you the most and I hope that you are proud of everything that I have accomplished here. I know that one day my younger brother and sister will read this thesis and be just as confused as I am writing it today about this thing called science.

I finally would like to thank my grandfather, who ironically stole my name. So, in way I thought concluding with a thank you to Malcolm was fitting to end these acknowledgments. I want to thank you for supporting me, persevering through the tough moments, and believing in me to achieve my goals. I am excited for new horizons.

Article IV. Contribution of Authors

All experiments in this thesis have been designed by me under guidance of my gracious supervisors Dr. Jonathan Spicer and Dr. Logan Walsh. S.M and F.B assisted with mice injections are takedowns. S.D, M.S, M.Y and L.D assisted with flow cytometry. M.M helped with neutrophil related experiments and R.R and V.B helped with all IF processing. S.M and S.Mc assisted with HALO analysis. All other analyses were done by me or in conjunction with relevant university research cores.

Article V. List of Tables and Figures

Tables

Figures

Article VI. List of Acronyms

AP – Activator Proteins

APC – Antigen presenting cell

CT – Computerized Tomography

CTC – Circulating tumor cells

DNA – Deoxyribonucleic Acid

ECM - Extracellular matrix

IL-10 - Interleukin-10

IL-8 - Interleukin-8

IMC - Imaging Mass Cytometry

LCNEC - Large cell neuroendocrine carcinoma

LDCT - Low dose computerized tomography

LUAD – Lung Adenocarcinoma

MMPs - Matrix metalloproteinases

MUACC - McGill University Animal Care Committee

NETs – Neutrophil Extracellular Traps

NLR – Neutrophil to Lymphocyte Ratio

NLST - National Lung Cancer Screening Trial

NSCLC - Non-small cell lung cancer

Pad4 - Peptidyl arginase deiminase 4

PAMPs - Pathogen-associated molecular patterns

PD1 – Programmed cell death protein 1

RBC – Red blood cells

ROS - Reactive oxygen species

SABR-BRIDGE – **S**tereotactic **AB**lative **R**adiotherapy **B**efore **R**esection to Avo**I**d **D**elay for Early-Stage Lun**G** Cancer or Oligom**E**ts

SARS-CoV-2 - Severe Acute Respiratory Syndrome Coronavirus 2

SABR – Stereotactic Body Radiation Therapy

T Regs - Regulatory T cells

TANs - Tumor-associated neutrophils

TIME – Tumor Immune Microenvironment

TLRs - Toll-like receptors

TME – Tumor Microenvironment

TNF-α – Tumor necrosis factor alpha

VATS - Video-assisted thoracoscopic surgery

VEGF - Vascular endothelial growth factor

OS – Overall survival

EFS – Event free survival

EGFR – Epidermal growth factor receptor

DFS – Disease free survival

pCR – Pathological complete response

Article VII. Background

Section 7.01 Introduction

(a) General introduction to Non-Small Cell Lung Cancer (NSCLC)

(i) Prevalence and significance of NSCLC

Lung cancer is the leading cause of cancer related mortality in Canada with 1 in 15 Canadians being diagnosed in their lifetimes [1]. Early-stage non-small cell lung cancer (NSCLC) - stage 1 and 2 - has a 5-year survival rate of 63% representing roughly 30% of cases. Worldwide lung cancer comes second in incidence among all cancer types and accounts for the largest loss of life [2].

(ii) Current treatment modalities and their limitations

Current standards of care for early-stage NSCLC include surgical resection and stereotactic ablative radiotherapy (SABR). Specifically, lobectomies entail the removal or an entire cancerous lobe of the lung while, resections – wedge, or segmental – only remove a portion of the lobe [3]. SABR aims to introduce a curative dose of ablative radiation to the tumor site and is generally used in patients that are inoperable [4]. Both treatment modalities have trade-offs. Surgery provides the benefit of definite diagnosis of the tumor including nodal staging, however, is relatively invasive in comparison to SABR and confers short term perioperative risks. In contrast, SABR is non-invasive and available studies suggest that it might provide similar effectiveness in comparison to surgery. However, locoregional recurrence, particularly with increasing tumor size continues to represent a major limitation for SABR to become the preferred standard of care for early-stage NSCLC [4].

(iii) The role of radiation therapy in NSCLC treatment

1) Mechanisms of action

In NSCLC treatment the key difference between SABR and conventional radiation therapy is that SABR delivers much larger doses of biologically significant radiation to the tumor site. This allows for more effective local control of tumors, comparable to surgical techniques [5]. Moreover, the advent of the severe acute respiratory syndrome coronavirus 2 (SARS-CoV-2) pandemic demonstrated the need to have effective treatment strategies that require minimal patient-doctor interaction as well as minimize utilization of key hospital resources such as operating rooms [6].

2) Challenges and issues related to radiotherapy.

There are several low-grade risks (1-2) associated with SABR including decrease pulmonary function and chest wall toxicity [5]. These parenchymal changes can make it difficult to assess disease response in treated patients. Further, unlike surgery, patients receiving SABR do not generally receive definitive nodal staging and experience low levels of locoregional reoccurrence and moderate rates of distant reoccurrence [5].

(b) Introduction to Neutrophil Extracellular Traps (NETs)

(i) What are NETs?

Neutrophil extracellular traps (NETs) are weblike DNA extrusions released from neutrophils at sites of chronic inflammation including the tumor microenvironment. The process of releasing NETs is termed NETosis and is hypothesized to be an alternative death pathway for neutrophils that performs antimicrobial properties during infection [7].

(ii) Functions of NETs in immune responses

Initially in response to inflammatory stimuli neutrophils are released into circulation and recruited to infected tissues where they play several roles. Namely, neutrophils will bind, phagocytose and inactivate bacteria [8]. NETs ameliorate this process by sequestering bacteria in their weblike structures allowing for high local dose of antimicrobial factors as well as forming a physical encapsulation – preventing further spread of any bacteria [8].

(iii) Relevance of NETs in cancer research

In NSCLC cancer, the neutrophil to lymphocyte ratio (NLR) is prognostic with a lower NLR being associated with better outcomes. Specially, NETs have been shown to both functionally and metabolically exhaust effector T cells, which are key immune drivers of cancer control that are harnessed with several treatment modalities including radiation, and immunotherapy [9]. Further, recent studies in bladder cancer have shown that radiation treatment increases the deposition of NETs in the tumor microenvironment and importantly inhibition of NETs improved response to therapy [10]. NETs have also been indicated in improving metastatic properties of tumors by providing a scaffold for tumors to metastasize and grow at distant sites suggesting that NETs may play a role in both loco-regional and distant metastasis [11].

(c) Objectives and Rationale

My project aims to characterize the impact of NETs in the tumor microenvironment (TME) on radiation efficacy in murine models. So far preliminary subcutaneous models show that inhibition of NETs leads to significant decreases in tumor volumes however this phenotype has not yet been observed in the setting of lung cancer. We hypothesize that Neutrophil Extracellular Traps (NETs) may play a role in radio-resistance by decreasing effector T cell infiltration in the

tumor immune microenvironment (TIME) and thus preventing immunogenic cell death resulting from SABR.

Section 7.02 Background on Early-Stage NSCLC

(a) Staging and classification of NSCLC

(i) Subtypes of NSCLC

NSCLC include three main subtypes: adenocarcinoma, squamous cell carcinoma, and large cell carcinoma [12]. Each of these histologies can be further stratified in several groups. Adenocarcinoma the most common subtype (40%) is extremely heterogenous and can be further subdivided into several groups: adenocarcinoma in situ, minimally invasive, invasive nonmucinous (lepidic, acinar, papillary, micropapillary, solid), invasive mucinous, colloid, fetal, enteric, and NOS adenocarcinomas [13]. Squamous cell carcinomas (25%) are characterized by morphological squamous cells and has been highly linked to smoking use in patients [14]. Lastly, large cell carcinomas (10%) can be divided into 5 subgroups: Large cell neuroendocrine carcinoma (LCNEC), basaloid carcinoma, lymphoepithelioma-like carcinoma, clear cell carcinoma, and large cell carcinoma with rhabdoid phenotype [12,14].

(ii) TNM classification system

As adenocarcinomas are heterogenous and present with different localizations and severity in patients, it is critical to have consistent classification for tumor stages to inform prognosis and treatment approaches. Recently, the eighth edition of TNM staging has been released to inform this process. TNM staging can be broken down into three components: characteristics of the primary tumor (T), involvement of the regional lymph nodes (N), and the presence of distance metastases [15]. Early-stage NSCLC can be defined as stages 1 and 2 and ranges from T1-2, N0-1,

and M0. When outlining tumor sizes the largest diameter is taken to stage appropriately [16]. In general, T1 staging for adenocarcinoma indicates a lepidic tumor size ≤ 3 cm located in or distal to the lobar bronchus with no local invasion [15]. The T1 stage can be further broken down in 4 substages: minimally invasive (mi), a, b, and c respectively. Tumor size increases with each substage and it outlined as the following: T1a (size ≤ 1 cm, T1b (1 cm < size ≤ 2 cm, and T1c (2 cm < size ≤ 3 cm). T1mi includes solid tumors that are ≤ 0.5 cm with the partly solid region not extending beyond 3cm total [16]. T2 staging is defined by any of these key characteristics: tumor size > 3 cm but ≤ 5 cm, invasion of the main bronchus, or presence of atelectasis or obstruction, pneumonitis of the hilar region, and local invasion (specifically visceral pleura) [15]. The substages of T2 (a, b) are similarly defined by increasing tumor size with T2a being from 3 cm < size ≤ 4 cm and T2b being 4 cm < size ≤ 5 cm [15]. In terms of nodal involvement, early-stage adenocarcinoma ranges from stage N0-1. Stage N0 can be defined as no regional lymph node involvement and stage N1 is characterized with involvement of the ipsilateral peribronchial and/or ipsilateral hilar lymph nodes [15,16]. Early-stage adenocarcinoma can be characterized as node negative and has an absence of distant metastases (TxN0M0) [15].

(b) Importance of early-stage detection

Advanced stage lung cancer has a poor 5 year survival rate of 21% compared to earlier stages [17]. As a result, while there is a need for developing new systemic therapies for advanced disease, is it imperative to have early detection strategies that allow for curative treatment modalities. The current standard for early detection is spinal low dose computerized tomography (LDCT) [18,19]. LDCT allows for scanning of the entire chest within a period of 15 seconds which provides convenience, accessibility and reduces the potential impacts of motion artefacts on the image result [19]. The National Lung Cancer Screening Trial (NLST) demonstrated that LDCT is

more superior to alternative screening strategies such as MRI at downstaging lung cancer patients that are at high risk [18,20]. However, many follow up studies in Europe and North America have not been able to replicate this effect mainly due to the limited inclusion criteria of NLST: high risk patients between 55-74 with a 30 pack-year smoking status [20-23]. Along with not being suited for assessment in low-risk patients, the drawbacks of NLST include false positive diagnosis, excessive radiation exposure, and medical costs [18,24]. As a result, there is a need for new non-invasive early detection tools, of which liquid biomarkers takes the forefront. Biomarkers would potentially be able to provide both early detection and diagnosis while also stratifying cancer risk based on malignancy [24-26].

(c) Treatment options for early-stage NSCLC

(i) Surgery

The primary curative treatment modality for patients that present with early stage (I & II) adenocarcinoma is surgical resection [27]. This is due to the large breadth of retrospective survival data that supports a moderate benefit in comparison to other treatment options, with a 5-year survival rate of 60-80% for stage 1 patients, and 30%-50% for stage 2 patients [3,12,27-29]. Patients' surgical eligibility depends on various patient-specific factors, including age, overall health, and pulmonary function as well as technical factors including whether complete resection of tumor and regional lymph nodes is possible [30]. In patients that are selected for surgery, prehabilitation, which involves optimizing a patient's physical and mental well-being before surgery is often used to reduce perioperative risks.

Historically, the surgical management of early-stage NSCLC has been characterized by the use of lobectomy, supported by the Lung Cancer Study Group Trial [28]. At the time the trial conclusively demonstrated the superiority of lobectomy over limited-lobe resections. However,

recently two studies have demonstrated the non-inferiority of wedge-resections and segmentectomies in comparison to lobectomies. JCOG0802 found that segmentectomies were superior to lobectomies in overall survival (94.3% versus 91.1%) despite seeing higher rates of local recurrence (10.5% versus 5.4%) and negligible differences in disease free survival [31]. CALGB140503 on the other hand demonstrated the efficacy of all sublobar resections (wedge and segmentectomy inclusive) in comparison to lobectomy, reinforcing the viability of these surgical options in early-stage NSCLC patients with node negative disease and tumors 2cm or smaller [32].

Additionally, surgical intervention has advanced with the incorporation of minimally invasive techniques, like video-assisted thoracoscopic surgery (VATS). VATS allows for precise resections through smaller incisions, leading to shorter hospital stays, and reducing postoperative complications and recovery time [27]. Further, VATS significantly enhances staging accuracy by providing a detailed view of the thoracic cavity [12,27]. This approach enables a thorough examination of the lung surface, lymph node's pleural involvement, and nearby structures, improving tumor characterization. As disease recurrence in patients that receive resection in not uncommon, VATS driven lymph node assessment allows for definitive lung cancer staging which can inform prognosis after surgery [5].

(ii) Stereotactic Body Radiation Therapy (SABR)

Stereotactic Body Radiation Therapy (SABR) has emerged as a definitive option for early-stage non-small cell lung cancer (NSCLC), supported by a growing body of research [4,6,33-35]. SABR is distinguished by its non-invasive nature and its ability to deliver highly targeted, high-dose radiation to tumors while sparing healthy surrounding tissue [6]. It has introduced a notable shift in the management of early-stage NSCLC, for patients who may not be suitable candidates for surgery due to factors like age, comorbidities, or impaired lung function [33]. SABR has

demonstrated impressive outcomes in terms of local control and survival rates. Local control rates frequently exceed 90%, showcasing its potent tumor-ablative capabilities [33]. Additionally, 5-year survival rates for patients treated with SABR have been reported to range between 50% and 70% for early-stage NSCLC [6,35]. Further, I-SABR – SABR used in conjunction with immunotherapy has been shown to significantly improve event free survival (EFS) at 4 years in comparison to SABR alone, highlighting the potentially of effective combination therapies [36]. These figures underscore the viability of SABR in achieving durable local control and favorable long-term survival outcomes.

SABR treatment approach is distinct in comparison to conventional radiation therapy. It utilizes advanced imaging techniques, such as CT scans and real-time imaging, to precisely locate the tumor in three-dimensional space [33].This high-level precision enables radiation oncologists to determine the exact coordinates of the tumor with exceptional accuracy. The concentrated high doses of radiation delivered with SABR are intended to effectively ablate the tumor [33]. This approach is particularly well-suited for small, well-defined tumors commonly found in early-stage NSCLC [35]. Further, in contrast to conventional radiation therapy, which typically involves daily treatments over several weeks with lower doses of radiation, SABR employs a hypo-fractionated approach [34].This means that a small number of high-dose radiation treatments are delivered, often over just a few sessions. The concentrated radiation dosage is strategically administered to maximize its impact on the tumor while minimizing exposure to healthy surrounding tissue [6]. Several SABR-specific changes in the TIME include inducing tumor cell death, increased anti-tumor immunogenicity, vascular reformation impacting tumor oxygenation and blood flow, and stromal remodeling, including ECM changes, angiogenesis, immune infiltration, and TIME signaling [6]. This is achieved through meticulous planning, real-time tracking, and the ability to

adapt treatment based on the tumor's position during each session. By sparing healthy tissue, SABR aims to reduce the risk of radiation induced side effects and preserve the patient's quality of life. Furthermore, fewer radiation sessions can reduce the logistical burden on patients and healthcare systems allowing patients to return to their daily lives quicker [4].

While SABR excels in local control, it's important to recognize that the likelihood of recurrence can vary based on several factors, including tumor size, location, and patient-specific comorbidities [33]. Recurrence rates following SABR typically range from 10% to 30% [35]. The risk of recurrence and the inability to accurately pathologically stage disease presents some of the current limitations in becoming the gold standard early-stage intervention. As a result, decisions regarding treatment should be made in consultation with a multidisciplinary team, considering the specific circumstances and preferences of the patient.

(iii) Systemic Therapies

Within the complex realm of early stage to NSCLC treatment, systemic therapies such as chemotherapy, immunotherapy, and targeted therapies provide a unique approach to enhancing cancer treatment effectiveness [5,12,29,37]. The main limitation of local treatment modalities including surgery and SABR is that there is a moderate risk of both local and distant recurrence as well as the reality that many patients present with micro-metastases in the lung that may be out of the scope of treatment [12,38]. Consequently, systemic therapies have been vigorously tested in the neoadjuvant and adjuvant setting to improve the outcomes for early and locally advanced NSCLC. The PACIFC trial established the effectiveness of adjuvant Durvalumab at improving OS in unresectable stage 3 patients who received concurrent chemoradiotherapy [39]. In the neoadjuvant setting, chemotherapy was previously established as standard of care for downstaging patient disease to increase the operability of tumors [40]. However, Checkmate 816 demonstrated a

superiority in EFS and pCR when using combination chemotherapy-nivolumab in these instances [41,42]. Further, Checkmate 77T seeks to elucidate if response durability can be improved when Nivolumab is additionally given in the adjuvant setting [43]. Several other trials including Aegean, Neotorch, and Keynote 671 have demonstrated similar effects of increasing EFS and pCR with the utilization of immunotherapy in either neoadjuvant or adjuvant settings [44-46]. In term of targeted therapies, for early stage patients with epidermal growth factor receptors (EGFR) mutations, Osimertinib was shown to increase disease free survival (DFS) [47]. Similarly, in patients with ALK showed comparable effects, demonstrating superiority to adjuvant chemotherapy in terms of DFS [48]. The usage of systemic therapies highlights one of the mechanisms of improving early-stage NSCLC outcomes as a significant number of patients will progress to advanced disease.

(iv) Challenges in treating early stage NSCLC

Effectively managing early-stage NSCLC presents a multifaceted challenge, specifically related to the complexities of tumor heterogeneity and recurrence rates. Tumor heterogeneity is a striking feature in early-stage NSCLC, encompassing a diverse array of genetic and molecular characteristics, such as histological subtypes, genetic mutations, and molecular variations [49]. Each tumor in unique – with even different regions of the tumor having distinct features, necessitating a precision medicine approach to the specific attributes of each patient's cancer. Moreover, the persistent risk of tumor recurrence, even following potentially curative treatments like surgical resection, is an unfortunate reality of current cancer care, demanding vigilant post-treatment surveillance, early detection methods, and adaptable strategies to address recurrent tumors that may exhibit different molecular profiles and treatment-resistant features [5].

The intricate landscape of early-stage NSCLC management also involves determining the optimal sequence and combination of therapies, making neoadjuvant and adjuvant treatments

important auxiliary elements of care [5,49]. Deciding when and how to deploy chemotherapy, immunotherapy, radiation therapy, or their combinations, requires a thorough evaluation of each patient's clinical and pathological specifics, underlining the importance of personalized treatment approaches that cater to individualized needs.

Moreover, although neoadjuvant and adjuvant chemotherapy and immunotherapy present the opportunity to improve survival rates, they have associated toxicities that can negatively impact patient quality of life [5,49]. Striking the right balance between patient wellbeing and treatment effectiveness is paramount in providing comprehensive care to early-stage NSCLC patients.

Addressing these multifaceted challenges requires the ongoing evolution of early-stage NSCLC management, with a focus on precision medicine, and a multidisciplinary approach to patient care [5,49]. The integration of innovative diagnostic techniques and therapeutic modalities plays a pivotal role in advancing early-stage NSCLC patient outcomes and the overall management of this heterogenous cancer type.

Section 7.03 Neutrophils in Cancer and Immunity

(a) Neutrophil functions in the immune system

(i) Phagocytosis

Neutrophils, integral defenders of the innate immune system, have been established as critical sentinels in the battle against microbial threats [50]. Characterized as front-line immune cells, neutrophil's phagocytic ability is imperative to the host immune defense strategy. Neutrophils work by deploying an arsenal of receptors and adhesive molecules, including Toll-like receptors (TLRs), complement receptors, and selectins, providing them with the unique ability to recognize and adhere to a wide array of microbial intruders [51]. For example, TLRs enable them to detect

pathogen-associated molecular patterns (PAMPs), facilitating swift responses to infections. The interaction between selectins and their ligands on endothelial cells is crucial for neutrophil rolling and adhesion during inflammation, paving the way for their migration towards sites of infection or tissue injury [52].

Following recognition and binding, neutrophils efficiently engulf pathogens. Once pathogens are enclosed, neutrophils unleash a barrage of antimicrobial peptides, enzymes, and reactive oxygen species. These mechanisms together create a hostile intracellular environment, rendering pathogens unable to survive within the neutrophils [53,54]. Moreover, this process can be enhanced when opsonins, such as immunoglobulins and complement proteins, bind to the pathogens, marking them. This molecular labeling significantly enhances neutrophils' ability to recognize and bind these marked invaders as neutrophils are equipped with receptors designed to specifically detect these opsonins. When engaged, this cascade triggers a rapid response and more effective clearance of the marked microbes. As a result, the opsonization process ensures the swift and efficient removal of a diverse array of microbial assailants [55]. This rapid reaction is instrumental in ensuring the timely elimination of bacteria, fungi, and other pathogens, thereby thwarting the dissemination of infections and minimizing potential tissue damage [50,56].

(ii) Release of inflammatory cytokines

Neutrophils, in addition to their central role in phagocytosis, are key players in fine-tuning immune dynamics through the release of pro-inflammatory cytokines. These cytokines wield substantial influence over immune responses, extending their impact beyond infection defense [57].

Activated neutrophils secrete tumor necrosis factor-alpha (TNF-α), a potent pro-inflammatory cytokine, which is pivotal in initiating and amplifying immune reactions. TNF-α, contributes to the recruitment and activation of other immune cells at sites of infection or

inflammation [54]. This cytokine is extremely dynamic and can recruit cell types such as neutrophils, macrophages, and monocytes to sites of infection, as well as enhance the ability of macrophages and neutrophils to phagocytose. Further, TNF-α catalyzes the expression of endothelial adhesion molecules, thereby facilitating the extravasation of immune cells from the bloodstream to the seats of infection [51,54]. Additionally, neutrophils serve as a source of interleukin-8 (IL-8), a chemokine known to act as a chemoattractant for other neutrophils, myeloid and lymphoid cells, as well as playing an important role in angiogenesis and immune cell activation [50,56].

The vast sphere of influence held by neutrophils also extends to adaptive immunity. Their release of pro-inflammatory cytokines can have significant impacts on the adaptive immune system. Notably, cytokines derived from neutrophils can steer the differentiation and activation of T cells, effectively modulating the adaptive immune reaction [54,57]. Neutrophils thus partake in a sophisticated interplay of immune interactions that fundamentally shape the broader immune response, underscoring their significance in fine-tuning both acute and chronic inflammation while maintaining immune equilibrium.

(b) Role of neutrophils in cancer progression

(i) Tumor-associated neutrophils (TANs)

Within the landscape of cancer progression, tumor-associated neutrophils (TANs) are multifaceted actors within the tumor microenvironment (TME). TANs play a dualistic role, influencing both tumorigenesis and immune responses. Through interactions with cells and structures in the TME as well as tumor cells, TANs confer both pro-tumorigenic and anti-tumorigenic effects [50].

One facet of TANs' pro-tumorigenic role centers on their ability to promote angiogenesis, a critical process for tumor growth and metastasis. Within the TME, TANs secrete pro-angiogenic factors, namely vascular endothelial growth factor (VEGF) and angiopoietin-1, which actively participate in the development of a vascular network. Tumors can leverage this vascular network to stimulate growth and funnel nutrients into the tumor bed. Further, intratumor vascular networks can be used as conduits for tumor cells to enter the bloodstream, facilitating metastatic spread [50,55]. In addition, TANs contribute to the remodeling of the extracellular matrix (ECM), releasing matrix metalloproteinases (MMPs), notably MMP-9. Specifically, MMP-9 aids in the breaking down of the ECM, enhancing cancer cell motility, and promotes invasive behavior into nearby tissues [50]. However, TANs also play a role in enhancing anti-tumor immune responses. TANs can act as antigen-presenting cells, facilitating the activation of cytotoxic T cells against cancer cells triggering the adaptive immune system to become anti-tumorigenic [50].

(ii) Neutrophil-mediated immunosuppression

While TANs exhibit both pro-tumorigenic and anti-tumorigenic roles, neutrophils can also impair the function of essential immune cells through various mechanisms creating an immunosuppressive environment within the TME [50]. The generation of reactive oxygen species (ROS) is one of these main factors. ROS are potent molecules capable of disrupting the functions of immune cells like cytotoxic T cells and dendritic cells through oxidative stress and cell structure modifications. The introduction of ROS into the TME weakens the immune system's ability to mount robust anti-tumor responses [56].

Further, neutrophils have the capacity to secrete immunosuppressive cytokines, expanding their contribution to immune suppression. Interleukin-10 (IL-10) is immunosuppressive cytokine produced by neutrophils which adversely affects cytotoxic T cells and natural killer cells,

diminishing their capacity to execute effective anti-tumor actions [56]. Further IL-10 can negatively impact the antigen presenting capabilities of antigen presenting cells (APCs) reducing anti-tumorigenic immune activation. The influence of neutrophils also extends to the modulation of regulatory T cells (Tregs), which possess potent immunosuppressive capabilities. By promoting the generation and activation of Tregs, neutrophils contribute to the reinforcement of the immunosuppressive setting within the TME, hindering anti-tumor immunity [55].

(c) Emerging role of NETs in cancer

(i) NET formation and composition

The formation of neutrophil extracellular traps (NETs) plays a crucial role in immune responses. When neutrophils encounter pathogens, inflammatory signals, or the heterogenous microenvironment of tumors, a unique form of cell death known as NETosis is triggered [58]. During NETosis, neutrophils undergo specific morphological changes, leading to the release of NETs, which are web-like DNA structures composed of chromatin, antimicrobial proteins, and enzymes [8]. In homeostasic conditions, NETs serve a dual purpose in immune defense, as they not only capture and immobilize pathogens but also deliver a lethal dose of antimicrobial agents.

The formation of NETs is characterized by the following steps: neutrophils are initially activated by various stimuli, such as bacterial components or proinflammatory cytokines, initiating a complex intracellular signaling cascade [59]. After that, peptidyl arginase deiminase 4 *(Pad4*), an enzyme endogenous to neutrophils will catalyze the conversion of arginine residues into citrulline on histone proteins [60]. This citrullination process promotes chromatin decondensation and allows the expulsion of chromatin from the neutrophil's nucleus, forming the structural backbone of NETs. During this process, other antimicrobial proteins and granule contents are mixed with the decondensed chromatin, creating a lethal cocktail for captured pathogens. In practice, the

antimicrobial function of NETs is twofold. Firstly, NETs create a physical barrier that entraps bacteria, fungi, and other microorganisms [11]. In addition, NETs are rich in antimicrobial molecules, including defensins, myeloperoxidase, and lactoferrin, which act in synergy to establish a hostile microenvironment for pathogens. This combination effectively immobilizes and kills microorganisms, thus preventing the spread of infections and supporting the body's defense mechanisms [61].

(ii) NETs in cancer metastasis

Recent literature has elucidated the increasing importance of Neutrophil Extracellular Traps (NETs) in the context of cancer metastasis, specifically, their capacity to both impede and facilitate the spread of cancer cells [62,63]. Their anti-metastatic potential lies in NETs ability to physically entrap cancer cells within the bloodstream, thus hindering their ability to travel to distant sites [61,63]. These intricate web-like structures act as a net, effectively capturing and immobilizing circulating tumor cells (CTCs), particularly in the microvasculature, which can substantially curtail the formation of secondary tumors. In contrast, NETs can also facilitate cancer cell extravasation, a pivotal step in metastasis, by providing a scaffold for cancer cells to adhere to in the endothelial lining of blood vessels [60]. This actively supports the successful transmigration of cancer cells into adjacent tissues. Furthermore, NETs can act as a protective shield for CTCs during their transitory period in the bloodstream, protecting them from immune surveillance and thereby enhancing their chances of survival and initiating metastasis at a distant site [59]. In the context of obesity neutrophil oxidative stress promotes NETs formation and induces vascular dysfunction enhancing cancer cell transmigration [64]. The delicate equilibrium between NETs' inhibitory and promotional roles in cancer metastasis hinges on several factors, including the distinct tumor microenvironment and the intricate interactions between cancer cells, immune cells,

and the vasculature. As a result, designing targeted therapy approaches to leverage NETs inhibitory approaches while mitigating pro-tumorigenic effects is essential.

Section 7.04 NETs in Radiation Response

(a) Introduction to NET-mediated radio-resistance

In recent years, our understanding of cancer therapy resistance has witnessed a remarkable shift, particularly in the context of radiation therapy. Radiation therapy's mechanism of action is to damage DNA within tumor cells to facilitate their death [65]. As a result, the phenomenon or radio-resistance – that is to say tumors that don't respond to conventional radiotherapy - was simply understood to be tumors that had intrinsic mechanisms of escaping that fate. However, emerging research has unveiled a complex interplay within the tumor immune microenvironment, uncovering the role of NETs in radio-resistance. As previously described NETs have been characterized in homeostatic conditions to have roles in innate immunity and thrombosis, whereas in the context of the TME have demonstrated both pro-tumorigenic and anti-tumorigenic effects [64,66,67]. Remarkably, they also can have negative impacts on cancer treatment and serve as a multifunctional barrier that can reduce radiotherapy efficacy [11].

(b) Mechanisms of NET-mediated radio-resistance

We now understand that there are several mechanisms through which NETs can impeded the effectiveness of radiation treatment. In the context of bladder cancer, Shinde-Jadhav and colleagues elucidate how NETs, form an intricate physical barrier that not only impedes the penetration of radiation but also acts as a shield that protect cancer cells from effector cells, reducing the therapeutic efficacy of radiation [10]. This effect can be further exacerbated by the simultaneous properties of NETs to accumulate in microvasculature, damaging vital organs and

facilitating the metastatic spread of tumor cells to distant sites [60]. Moreover, research by Kaltenmeier and colleagues introduces a new dimension by characterizing the role of NETs in promoting T cell exhaustion within the tumor microenvironment [68]. T cell exhaustion can impede the immune system's ability to target and eliminate cancer cells leading to poorer responses to therapy.

Section 7.05 Significance of NETs in early-stage NSCLC

(a) Exploring the link between NETs and radiation response

The importance of addressing NET-mediated radio resistance is highlighted in the treatment of early-stage NSCLC. Radiotherapy provides a curative non-invasive approach to treatment which is not limited by the perioperative risks of surgical resection [33]. However, as about a third of patients experience reoccurrence it is critical to address factors that can impact radiation efficacy [41]. NETs seemingly are one of these bad actors that in early-stage NSCLC may reduce the potency of radiation but importantly also prime the TME for adjuvant therapy resistance in the context of T-cell exhaustion.

(b) Clinical implications

Recently researchers have been exploring innovative strategies to surmount NET-mediated radio resistance. Notably, the inhibition of peptidyl arginase deiminase 4 (*Pad4*), an enzyme pivotal in NET formation, has emerged as a promising avenue [69]. The use of GSK484, an inhibitor of *Pad4*, not only increases radiosensitivity in colorectal cancer but also effectively inhibits the formation of NETs [69]. The use of *Pad4* inhibition in tandem with radiation treatment for patients with early stage- NSCLC presents a promising avenue for NET elimination, thus enhancing the effectiveness of radiation therapy.

Section 7.06 Research Gaps and Objectives

(a) Identification of knowledge gaps in the field

So far, we know that in bladder and colorectal cancer radiation increases deposition of NETs in the TME, subsequently, reducing the effectiveness of treatment [10,69]. In the context of NSCLC, preliminary subcutaneous murine models show that inhibition of NETs leads to significant decreases in tumor volumes, however, this phenotype has not yet been observed in an orthotopic setting. The immune landscape of the lung is drastically different from other tissues and as a result it is imperative to characterize NETs function in this environment.

(b) Research objectives and hypotheses

My project aims to characterize the impact of NETs in the tumor microenvironment (TME) on radiation efficacy in murine models. We hypothesize that Neutrophil Extracellular Traps (NETs) may play a role in radio-resistance by physically decreasing T cell infiltration and activation in the tumor immune microenvironment (TIME).

Section 7.07 Significance of the Study

(a) Potential impact of the research on NSCLC treatment

By delineating the precise mechanisms behind NET-induced radio resistance, future neoadjuvant therapies can be tailored to sensitize lung cancer cells to radiation, potentially amplifying the curative potential of radiotherapy in early-stage NSCLC. Further, the implications of increasing the effectiveness of SABR include broadening the global accessibility of early-stage lung cancer treatment through reducing the number of hospital visits, resources for perioperative care, and bypassing limited access to surgical facilities for many communities.

(b) Contribution to the understanding of the role of NETs in cancer

Neutrophil extracellular traps are unique elements of the TME. Unlike other cell types that may be harnessed by cancer cells to become pro-tumorigenic, NETs are “impartial” physical structures that accumulate at sources of inflammation becoming either scaffolds for tumor expansion or cages stifling their growth. As a result, characterizing how NETs function in the immune-privileged lung microenvironment is critical in understanding both cancer development and metastasis, as well as the morbidity of a variety of other inflammatory pulmonary diseases.

Section 7.08 Conclusion

Lung cancer is the leading cause of cancer related mortality in Canada with 1 in 15 Canadians being diagnosed in their lifetimes. Non-small cell lung cancer, specifically, adenocarcinoma makes up the largest subtype and is characterized by extreme tumor heterogeneity and poor advanced disease survival. For early-stage patients’ mainstays in treatment include lobectomy and radiation for those deemed inoperable. Radiation treatment is non-invasive compared to surgery; however, many patients recur limiting its universal applicability. Recently, neutrophils and their extrusions - termed neutrophil extracellular traps - have been indicated in modulating radiation response, conferring resistance. While other cancer types have established this relationship it is unclear if they same dynamics are at work in the lung tumor microenvironment as it is drastically different from other tissue types from both a structural and immune landscape standpoint. Here we seek to elucidate these processes through testing the impact of NET inhibition on the tumor immune microenvironment in orthotopic lung cancer murine models.

Article VIII. Methodology

Section 8.01 Animals and in vivo cancer models

All animal experiments were performed in accordance with the McGill University Animal Care Committee (MUACC). C57BL/6 (Charles River) and peptidyl arginine deiminase type IV knockout (*Pad4-/-*) (Pittsburgh, Allan Tsung's Lab) between the age of 7-10 weeks were used for all in vivo experiments. Experimental lung primary tumors were achieved with the orthotopic injection of 50 thousand LLC1 or HKP1 tumor cells into the lung. During this procedure, a left thoracic incision through the skin was performed and cancer cells were injected into the left lung. The cells were mixed with Matrigel Matrix (Corning) at a 1:1 vol./vol. ratio and injected at a volume of 20 µL. Animals then received an ablative dose of local irradiation 7 days post injection and were euthanized 10 to 15 days later depending on progression unless otherwise specified. Lungs were harvested and separated equally for histological and flow cytometry analysis. Additionally peripheral blood was collected in some instances for flow cytometry analysis. In cases where mice were treated with DNAse (Biomatik), 50uL of reconstituted solution as indicated by product protocols was injected intramuscularly. *InVivoPlus* anti-mouse PD-1 (Bio-Cell) was used in conjunction with the *InVivoPlus* polyclonal Armenian hamster IgG (Bio-Cell) to conduct all ICI trials. 100uL of antibody was injection per mouse at 33uL of antibody and 67uL of dilutant for the PD-1 inhibitor and 26uL of IgG vehicle with 74uL of dilutant.

Section 8.02 X-Rad Irradiator

Mice were irradiated with the X Rad SMART – Precision X-Ray. Mice were anesthetized and 8 Gy of radiation was delivered to each side of the mouse (rotated 180 degrees) using the settings 225 kV, 13 mA, 0.3 mm copper filter and a 1mm x 1mm colorimeter. Overall, this delivered a total ablative dose of 16 Gy locally to the tumor bearing lung of experimental mice.

The rationale for 2 fractions of 8 Gy was determined in consultation with the radiology department at the MUHC as a biological relevant ablative dose of radiation for mouse preclinical models.

Section 8.03 Histological Slide Preparation and Immunostaining

Harvested lungs were inflated and fixed with formalin for 24 hrs. Then, the lungs were stored in 70% ethanol until the cassettes were sent to the Histology Core of McGill university or the MUHC Glen site. 5 sections were then cut (10 micrometers apart) per cassette with 4 being using for immunofluorescence and one being used for H&E staining prepared by the histology core. Immunofluorescent staining was prepared on sections that underwent deparaffinization and antigen retrieval using the Ventana Discovery Ultra automated slide preparation system. The tissue sections were then washed 3 times for 2 minutes in PBS and outlined with a hydrophobic pen (PAP). Tissues were blocked with DAKO blocking reagent (1 hour at room temperature; Agilent). Primary antibodies were diluted in DAKO antibody diluent and incubated overnight at 4ºC (see antibody clones and concentration in **Table.1**). Tissues were rinsed 3 times in PBS, incubated for 1 hour at room temperature with AlexaFluor secondary antibodies (1:500, Invitrogen), and rinsed in PBS. DAPI (4,6-diamidino-2-phenylindole) was used to counterstain. DAKO fluorescent mounting media was added to the tissue sections and the coverslip was placed. After 1-2 hours at room temperature, the slides were stored in the dark at 4ºC. An Axio Scan.Z1 (Zeiss) and HALO (PerkinElmer) were used for quantification. Full slide sections were scanned with the Axio scan. Z1 and tumour burden, cell frequency and interactions where quantified with HALO algorithms *Indica Labs – CytoNuclear v2.0.9, Indica Labs – Highplex FL v4.04* and *Indica Labs – Object Colocalization FL v1.0* respectively. Tumor burden was characterized by classifying thresholds for intense basophilic cells allowing for separation of tumor cells from healthy cells in the tissue. For cell frequencies, 'Positive' cells were determined by creating a threshold for fluorescence intensity;

therefore, a ‘negative’ cell could result from an absence of the target protein or low levels of the target protein below the threshold. To determine colocalization of certain cell types and structures, expression level thresholds were used to identify specific cell types of interest.

Section 8.04 Table 1: Immunofluorescence Antibodies

Marker – Colour	Dilution	Supplier	Cat #	Host
CD8 – A594	100	Abcam	Ab217344	Rabbit
H3Cit – A594	100	Abcam	Ab5103	Rabbit
MPO – A647	100	R&D Systems	AF 3667	Goat
CD4 – A594	100	Novis Biologicals	AF 554	Goat
CD3 – A488	100	Abcam	Ab56313	Rat

Section 8.05 Flow Cytometry

Lungs were harvested and minced using a razor blade, rinsed with FACS buffer (dPBS + 2%FBS) and filtered through a 40µm cell strainer. RBC lysis (BD) was performed for 15min in the dark on the samples and then cell suspensions were centrifuged for 15min at 360Xg (no breaks) to enrich the leukocyte fraction of the samples. The cells were resuspended in dPBS containing live/dead stain and stained for 30 min at room temperature in the dark. Then, a combination of fluorochrome-conjugated antibodies at optimized concentrations in a 1:1 FACS to BV stain buffer (BD) for 30 min at 4 degrees Celsius. Samples were fixed with Fix/Perm solution (eBioSciene) for 1 hour at 4 degrees Celsius. Samples were acquired within 7 days of processing on a 4-lasers Cytek

Aurora Spectral Flow Cytometer. FlowJo v10.8.1 was used to analyze the acquired data. The following antibody panel was used:

Section 8.06 Table 2: Flow Cytometry Antibodies and Dilution Factors

Marker – Colour	Dilution	Supplier	Cat #	Clone
CCR2-BV421	200	BD Biosciences	747963	475301
CD103-Pacific Blue	100	BioLegend	121418	2E7
SiglecF-BV510	200	BD Biosciences	740158	E50-2440
CD11b-BV570	100	BioLegend	101233	M1/70
CXCR2-BV650	200	BD Biosciences	747813	V48-2310
CX3CR1-BV711	200	BioLegend	149031	SA011F11
CD11c-BV750	200	BioLegend	117357	N418
CD64-FITC	200	BioLegend	139316	X54-5/7.1
MHCII-Spark Blue 550	200	BioLegend	107662	M5/114.15.2
CD45-PerCP	100	BioLegend	103130	30-F11
Ly6G-PerCP eF710	200	Invitrogen	46-9668-82	1A8-Ly6g
CD24-PE	100	BD Biosciences	553262	M1/69
CD3-Spark YG 570	400	BioLegend	100266	17A2
CD8-Spark NIR 685	200	BioLegend	100782	53-6.7

CD19-PE-Cy5	100	BioLegend	115510	6D5
CD4-PE-Fire700	200	BioLegend	100484	GK15
F4/80-PE-Cy7	100	BioLegend	123113	BM8
Ly6C-AF647	200	BioLegend	128010	HK1.4
Zombie red	1000	BioLegend	423110	
Nk 1.1-APC	400	BioLegend	108709	PK136

Section 8.07 Clinical Cohort

A cohort of 25 of early-stage NSCLC patients were included in this study. Patients were subdivided into three groups: treatment naïve, chemotherapy + radiation, and SABR-Bridge. The SABR-Bridge group include patients that received neoadjuvant radiation before resection due to inaccessibility of operating rooms during the SARS-COV-2 pandemic. For each patient samples of the tumor were obtained following surgical resection. Tissue microarrays were constructed by taking multiple 1-mm^2 cores from the surgical tumor section. (MP-37-2021-6596, *SABR-BRIDGE*).

Section 8.08 Sample Staining and IMC

The protocol for sample staining has been previously described [70] but will be described briefly. Patient derived formalin-fixed paraffin-embedded FFPE slides underwent deparaffinization at 70 °C (Roche Diagnostics' EZ Prep solution). Subsequently, antigen retrieval was conducted at 95 °C using the standard cell conditioning 1 solution (Roche Diagnostics). The Ventana Discovery Ultra auto-stainer platform from Roche Diagnostics was used for this antigen retrieval step. Following these initial steps, the slides were rinsed with 1× PBS and subjected to a

45-minute incubation in DAKO serum-free protein block solution (Agilent). The slides were then stained with a cocktail containing metal-tagged antibodies. Antibodies were previously optimized on control tissues such as the spleen, tonsil, thymus, normal lung, and LUAD. This staining process occurred overnight at 4 °C. All antibody conjugations were performed by the team at the Single Cell and Imaging Mass Cytometry Platform at the Goodman Cancer Institute, McGill University, using Fluidigm's Maxpar Conjugation Kits for accuracy. Post-staining, the slides underwent rigorous washes and were treated with a secondary antibody cocktail comprising metal-conjugated anti-biotin. After a timed 1-hour incubation, slides were washed again. To prepare the slides for Imaging Mass Cytometry (IMC) acquisition, a counterstaining process was executed using Fluidigm's Cell-ID Intercalator-Ir at a specified dilution of 1:400 in 1× PBS, ensuring consistent and uniform counterstaining. IMC imaging was carried out with an approximate resolution of 1 μm, employing the Fluidigm Hyperion Imaging System. Laser ablation, a critical component of the imaging process, occurred at a frequency of 200 Hz. Subsequently, all raw data were compiled using Fluidigm's proprietary commercial acquisition software, maintaining data management throughout this methodological workflow.

Article IX. Results

Section 9.01 *Pad4* modulates the efficacy of Radiation Treatment in Early NSCLC Murine Models

In order to elucidate the impact of NETs on radiation response, we designed a trial that explored the response of C57BL/6 mice vs. *Pad4-/-* (a NET deficient strain) to ablative radiation treatment (Fig 1). At endpoint all irradiated mice had a decreased trend in tumor volume and weight in comparison to non-irradiated controls and female mice had slower tumor progression surviving

until 22 days compared to 17 days for males (survival difference by sex; p-value = 0.0037, Fig 1, Fig 2. A, B, C, Fig 5). When evaluating tumor burden in male mice, *Pad4-/-* mice that received radiation had the lowest resulting tumor burden in comparison to both treatment naïve *Pad4-/-* and C57BL/6 mice (25.1% vs. 63.6%, 43.8%, and 34.3% respectively, *Pad4-/-* vs. *Pad4-/-* + Radiation; p-value = 0.0116, Fig 3). This was consistent with a nonsignificant trend of increased expression of H3Cit (NET marker) and MPO (Neutrophil marker) in untreated C57BL/6 mice (Fig 4). When exploring the immune landscape of these mice we discovered that in female mice there was a significant increase in B cell abundance in female irradiated *Pad4-/-* mice in comparison to both treatment naïve and irradiated C57BL/6 mice (36.3% vs. 9.8%, and 18.7% respectively, ♀ *Pad4-/-* + Radiation vs. ♀ C57BL/6; p-value < 0.0001, ♀ *Pad4-/-* + Radiation vs. ♀ C57BL/6 + Radiation; p-value < 0.0001 , Fig 6.A). The difference between irradiated *Pad4-/-* mice and treatment naïve *Pad4-/-* mice was statistically nonsignificant, however, irradiated *Pad4-/-* mice trended towards having more B cells (36.3% vs. 29.1%, ♀ *Pad4-/-* vs. ♀ *Pad4-/-* + Radiation; p-value = 0.201, Fig 6.A). This was accompanied by a decrease in T cell abundance in only female *Pad4-/-* treatment naïve mice suggesting an expansion of the lymphoid compartment in the female irradiated *Pad4-/-* treatment group (23.5% vs. 38.7%; p-value = 0.0005, Fig 6.A). No changes in neutrophils or monocytes were observed in the female mice (Fig 6.A). Within the T Cell niche, CD4+ T cells where upregulated in the female irradiated C57BL/6, *Pad4-/-*, and *Pad4-/-* + radiation groups in comparison to the female C57BL/6 treatment naïve group (3.3% vs. 10.9%, 10.9%, and 8.8% respectively, ♀ C57BL/6 vs. ♀ C57BL/6 + Radiation; p-value < 0.0001, ♀ C57BL/6 vs. *Pad4-/-*; p-value < 0.0001, ♀ C57BL/6 vs. *Pad4-/-* + Radiation; p-value = 0.0009, Fig 6.B). However, there were no significant changes between these three upregulated groups (Fig 6.B). In the CD8+ T cell compartment, radiation increased CD8 T cell infiltration in female

C57BL/6 mice in comparison to treatment naïve mice (13.1% vs. 2.5%; p-value <0.0001, Fig. 6.B). Interestingly these same dynamics were not apparent in matched *Pad4*-/- mice (8.3% vs. 7.0%; p-value = 0.940, Fig. 6.B). Further, CD8 + T cell abundance was significant increased in irradiated female C57BL/6 mice in comparison to both treatment naïve and irradiated *Pad4-/-*mice (p-values = 0.0022, 0.0064 respectively), suggesting that in female mice, *Pad4* knockout decreased CD8 T cell infiltration. Overall, female *Pad4-/-* mice had a higher baseline level of CD8 + and CD4 + T cells in comparison to C57BL/6 mice and an increased B cell phenotype when treated with irradiation.

In male mice there was contrasting phenotype. Male *Pad4-/-* mice had decreased B cells in comparison to C57BL/6 controls (18.1% vs. 31.2% respectively; p-value = 0.0036). Further, in male C57BL/6 mice, radiation increased B Cell abundance in comparison to treatment naïve groups, while having no statistically significant effect in *Pad4-/-* irradiated mice (31.2% and 49.8%; p-value = 0.0001 vs. 18.1% and 25.1%; p-value = 0.185 respectively, Fig 7.A). In addition, there was a massive shift in the T cell compartment between male C57BL/6 mice and *Pad4*-/- mice. *Pad4*-/- mice on average had less T cells in treatment matched groups (♂ C57BL/6 vs. ♂ *Pad4*-/-, 50.5% vs. 14.9%; p-value < 0.0001, ♂ C57BL/6 + Radiation vs. ♂ *Pad4-/-* + Radiation, 54.3% vs. 28.3%; p-value < 0.0001, Fig 7.A). However, in *Pad4-/-* mice, radiation was still sufficient to increase T cell abundance (p-value = 0.0013). There were no statistically significant changes in neutrophils or monocytes, however, *Pad4-/-* trended towards having higher numbers of both cell types (Fig 7.A). In the T cells compartment we saw a slight increase in CD4+ T cells in the irradiated *Pad4-/-* treatment group in comparison to treatment naïve *Pad4-/-* mice (9.6% vs. 5.4% respectively; p-value = 0.0083, Fig 7.B). This dynamic was not present in the C57BL/6 cohort suggesting that *Pad4* knockout increased CD4 + T cell infiltration (Fig 7.B). Interestingly,

in contrast to female mice, CD8+ T cells were upregulated in male *Pad4-/-* that received radiation in comparison to both treatment naïve *Pad4-/-* mice as well as C57BL/6 groups (irradiated *Pad4-/-*: 9.5% vs. 4.5%; p-value = 0.0015, 4.2%; p-value = 0.0024, 3.6%; p-value = 0.007, in *Pad4-/-*, C57BL/6 and C57BL/6 + radiation respectively; Fig 7.B). This significant increase in CD8+ T cells in irradiated *Pad4-/-* mice was sex specific as we saw a contrasting decrease in female mice of the same condition. As a result, we wanted to dive deeper in order to comprehensively explore the immune microenvironment of male *Pad4-/-* mice who demonstrated both significant decreases in tumor burden as well as an increase in cytotoxic T cells when treated with radiation (Fig 3, Fig 7.B). However, due to the strong tumor burden phenotype we observed and the potential that at longer timepoints the adaptive and innate immune response may resolve, we sought to explore these dynamics at an earlier timepoint after radiation.

Section 9.02 Activated T Cells are Correlated with Improved Response Rates in irradiated *Pad4-/-* Mice

In order to evaluate the immune landscape during the radiation induced immune response we sought to explore immune dynamics at an earlier timepoint in male mice. We additionally used a DNAse model of NET inhibition to either establish an orthogonal method of radiation improvement or to determine if the improved response phenotype was *Pad4* dependent (Fig 8). At endpoint, all lungs presented with small, localized tumors, however, histological tumor burden analysis showed that the irradiated *Pad4-/-*mice had the smallest (25.1) percent tumor in the lung (Fig 9.A, B). In terms of tumor weights there were no significant changes between groups, however, on average *Pad4-/-* lungs were heavier at endpoint (Fig 9.C). When looking at the number of neutrophils that are NETosing in the lung, characterized by the colocalization of MPO (neutrophil marker) with H3cit (NET marker), we observed increased NETosis in irradiated

C57BL/6 lungs in comparison to *Pad4-/-* treatment naïve lungs (0.78% vs. 0.08% respectively; p-value = 0.0339 Fig 10.B). Further, when looking in the tumor bed CD8+ T cells were elevated in both irradiated C57BL/6 and *Pad4-/-* mice in comparison to relevant controls (77.6% vs. 31.8%; p-value = 0.094, 57.6% vs. 20.1%; p-value = 0.723 respectively, Fig 10.A, B). However, in the case of *Pad4-/-* mouse CD8 + T cell infiltration, only 2 residual tumors were present in 5 lung samples lending to the efficacy of *Pad4* knockout in combination with radiation but limiting the power of this relationship.

In terms of leukocyte distribution, both *Pad4-/-*treatment naïve and radiation treated groups experienced an elevation of lymphocytes in comparison to their corresponding C57BL/6 controls (64.4% vs. 38.7%; p-value < 0.0001, 51.8% vs. 37.9%; p-value = 0.0122 respectively, Fig 11). This lymphoid increase was accompanied my similar decrease in myelocytes for *Pad4-/-* groups (33.6% vs. 60.6%; p-value < 0.0001, 46.0% vs. 61.4%; p-value = 0.0040 respectively, Fig 11). In contrast, only the treatment naïve DNase treated group shared this phenotype (p-value <0.0001 and p-value <0.0001 for lymphocytes and myelocytes respectively, Fig 11). Trends present only in *Pad4-/-* and DNase treated groups were a decrease in lymphocytes and increase of myelocytes with irradiation (*Pad4-/-*: lymphocytes; p-value = 0.0240, myelocytes; p-value = 0.0260, DNase: lymphocytes; p-value = 0.0413, myelocytes; p-value = 0.0498, Fig 11).

When exploring the myeloid compartment, we discovered that irradiated *Pad4-/-* mice (11.1%) had a significant decrease in neutrophils in comparison to irradiated C57BL/6 mice (23.0%; p-value = 0.0211, Fig 12.E). Monocytes were upregulated in irradiated *Pad4-/-* mice in comparison to all other groups aside from *Pad4-/-* treatment naïve mice and irradiated DNase treated mice which was trending towards significance (p-value = 0.0618, Fig 12.D). For other

myeloid populations including macrophages, and natural killer cells there were no consistent changes between groups (Fig 12.A, B, C).

B cells were elevated in DNase treated groups, however, there was no difference with radiation treatment (p-value > 0.999, Fig 13.A). Unlike at day 18, at day 12 we saw no changes in B cell abundance between C57BL/6 and *Pad4-/-* groups (Fig 13.A). In terms of T cell distributions, radiation treatment in *Pad4-/-* and DNAse treated mice resulted in a small elevation of T cells in comparison to their corresponding treatment naïve groups, however, this increase was not statistically significant (45.7% and 42.9%; p-value = 0.999 vs. 40.7% and 39.3%; p-value = 0.999 respectively Fig 13.B). In general, CD4+ T Cell were downregulated in irradiated treatment arms (Fig 13.C). Specifically, irradiated *Pad4-/-* mice (35.67%) had significantly decrease CD4+ T cells in comparison to C57BL/6 mice (51.10%; p-value = 0.0335, Fig 3.I). In addition, this trend was consistent between *Pad4-/-* mice (35.67%) and both DNase treated groups (53.2%, 51.4%; p-values = 0.0002, 0.0014 respectively, Fig 13.C), suggesting different immune effects due to radiation in *Pad4-/-* vs. DNase treated NET inhibition models. Broad T cell changes were also consistent with an expansion of the CD8+ T cell compartment where we see a similar trend in C57BL/6, *Pad4-/-*, and DNAse treated groups (43.1%, 39.9%; p-value > 0.999, 39.4% vs. 37.5%; p-value = 0.879, and 35.5%, and 37.5%; p-value > 0.999 respectively, Fig 13.D). However, when we look at PD1+ CD8+ T cells only irradiated *Pad4-/-* mice (10.5%) were significantly elevated in comparison to all other treatment groups (p-value = 0.0002, Fig 13.E). This was further highlighted when looking at the neutrophil to lymphocyte ratio (NLR) as well as the neutrophil to PD1+ CD8+ T cell ratio where irradiated *Pad4-/-* mice ranked the lowest compared to other groups (0.3; p-value = 0.583 and 0.5; p-value = 0.0005 respectively, Fig 14.A, B). To see if these immune phenotypes could be recapitulated with unsupervised clustering, we constructed a PhenoGraph that

reinforced these relationships; namely the presence of a CD8+ T cell population upregulated only in irradiated *Pad4-/-* mice (Fig 15). The presence of this population of PD1+ cytotoxic T cells led us to explore if it was possible to leverage an increased immune infiltrate to improve the efficacy of adjuvant immune harnessing therapies such as immune checkpoint blockade.

Section 9.03 Immune Checkpoint Blockade was more effective in Irradiated *Pad4-/-* Mice

Next, we sought to test if these elevated PD1+ CD8+ T Cells that we see in irradiated *Pad4-/-* mice had any impact on ICI efficacy. The trial was designed such that after being irradiated on day 7, C57BL/6 and *Pad4-/-* mice were then treated with either a PD1 inhibitor or IgG vehicle (Fig 16). The primary endpoint of this trial was survival, with lungs being collected at endpoint for future histological analysis. In terms of gross lung appearance, localized or extra thoracic tumors were qualitatively present in all treatment groups except for irradiated *Pad4-/-* mice that received PD1 treatment (Fig 17.B). For survival, mice of either strain that received IgG vehicle instead of PD1 had a median survival of 21 days (C57BL/6: 20 days, *Pad4-/-*: 22 days, Fig 17.A), which was consistent with our previous trials (Fig.1). However, when treated with PD1 inhibitor, irradiated C57BL/6 mice lived longer, with a median survival of 28 days (27.5, Fig 17.A). Irradiated *Pad4-/-* mice had the most impressive survival and 80% of the cohort lasted until the endpoint of the trial, which was significant in comparison to both mice that received IgG vehicle and C57BL/6 mice that also received radiation (p-value = 0.0042 Fig 17.A). This demonstrates the efficacy of *Pad4* knockout in the context of improving adjuvant ICI after SABR in preclinical models.

Article X. Figures

Section 10.01 Figure 1: Trial Workflow Schematic

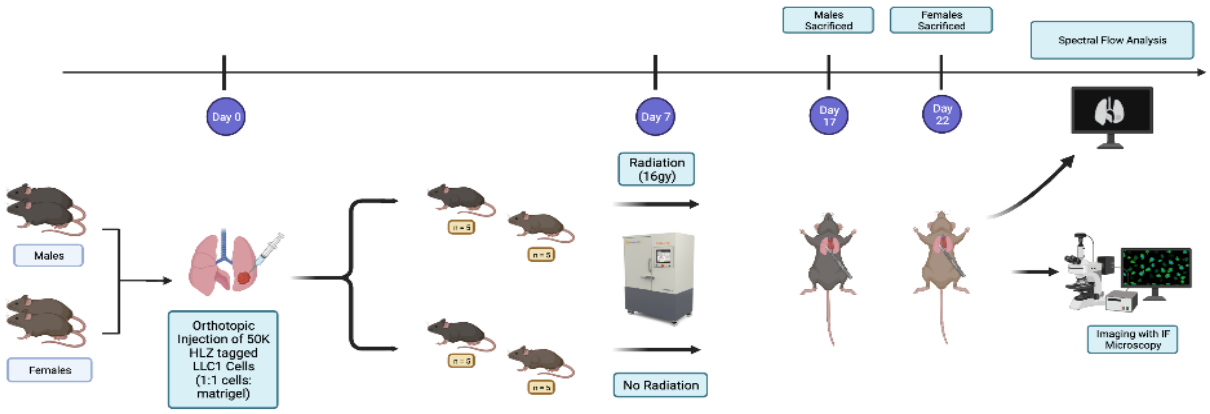

Fig 1: Schematic depicting trial workflow.

Section 10.02 Figure 2: Tumor Characteristics

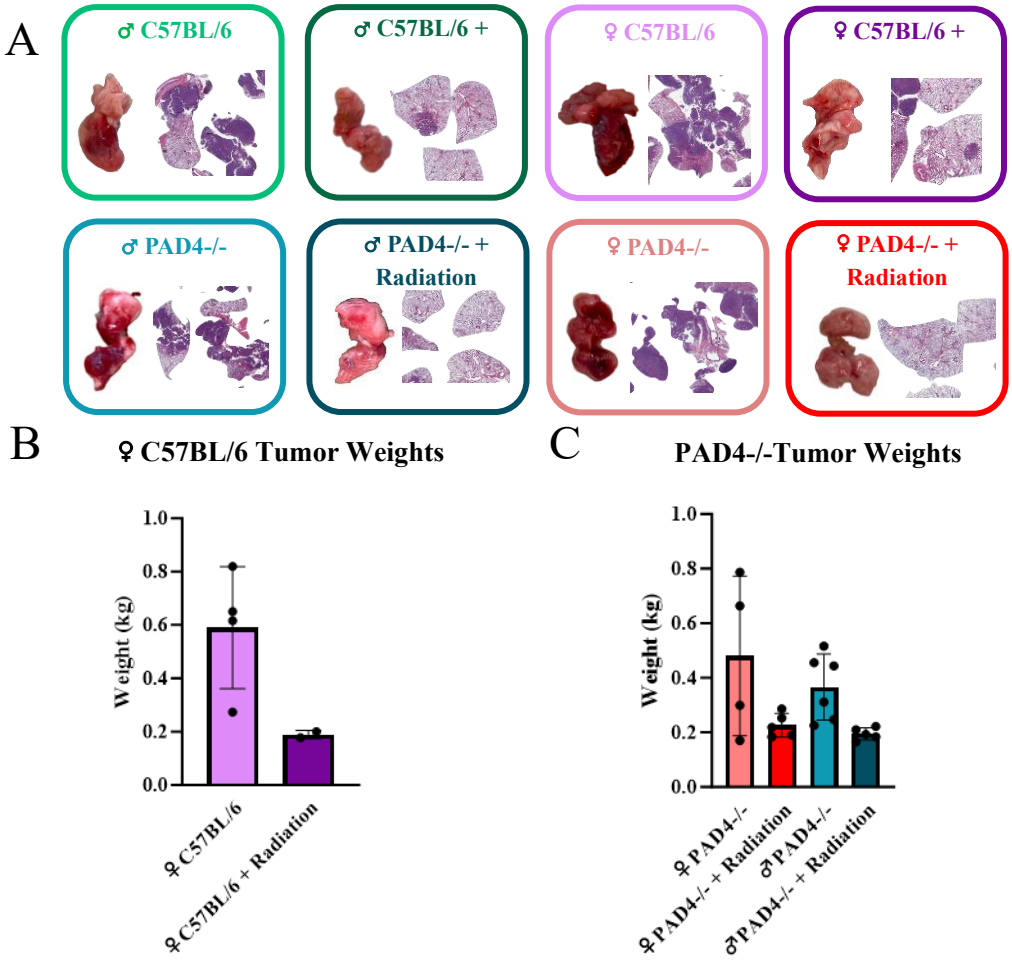

Fig 2: A. Representative lung images and histological H&E scans at end point for each treatment group. B, Female C57BL/6 (n=5) and Female C57BL/6 + radiation (n=5) lung tumor weights. C, Tumor weights of female *Pad4-/-* (n=5), female *Pad4-/-* + radiation (n=5), male *Pad4-/-* (n=5), and male *Pad4-/-* + radiation (n=5).

Section 10.03 Figure 3: Tumor Burden Analysis

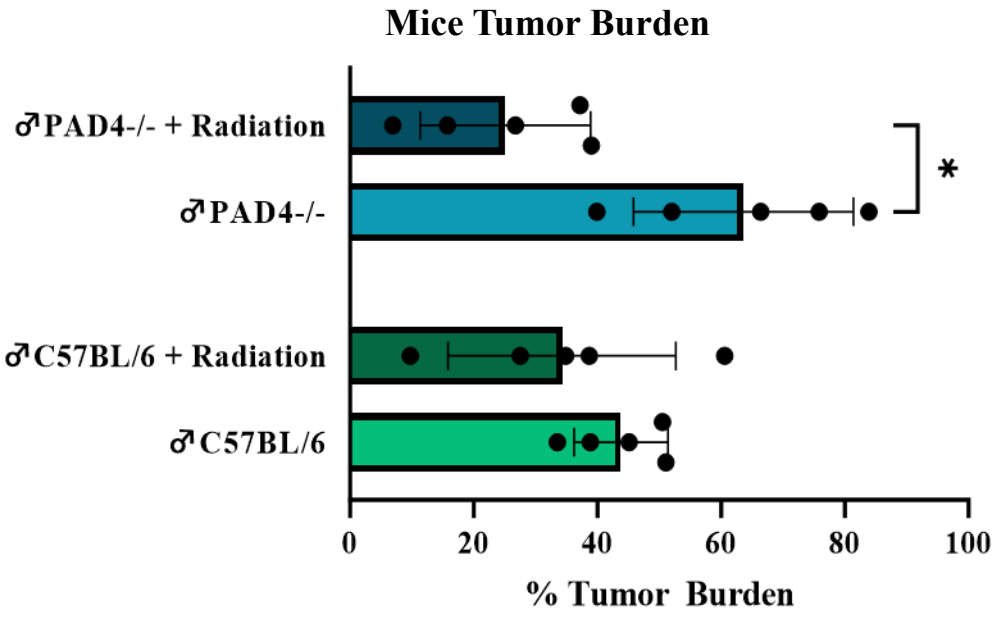

Fig 3: Tumor burden comparison between male treatment groups including C57BL/6 (n=5), C57BL/6 + radiation, *Pad4-/-* (n=5), and *Pad4-/-* + radiation.

Section 10.04 Figure 4: Immunostaining of NETs

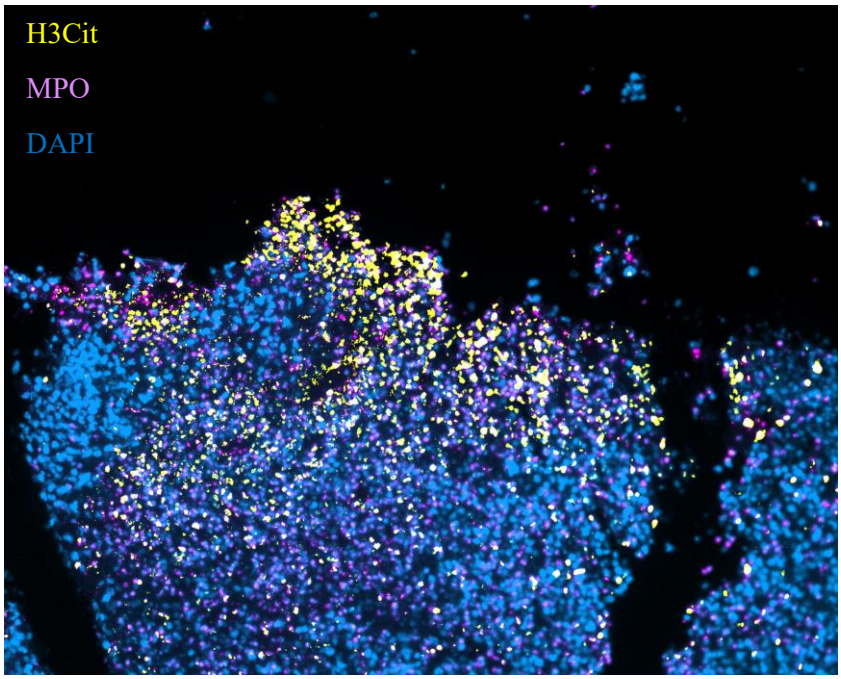

Fig 4: Representative immunofluorescence stain of H3Cit and MPO on C57BL/6 irradiated tissue.

Section 10.05 Figure 5: Survival Statistics

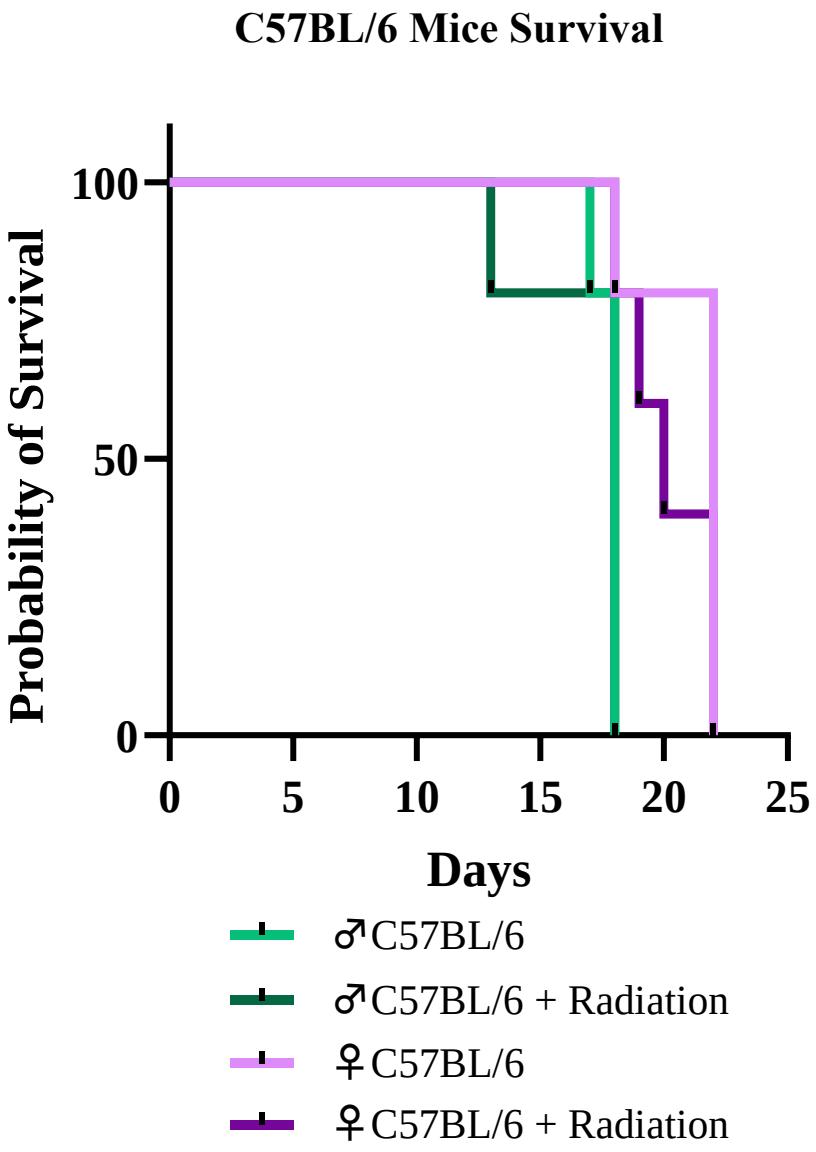

Fig 4: Kaplan Meier Survival plot of C57BL/6 treatment groups (n=10).

Section 10.06 Figure 6: Female Flow Cytometry Characterization

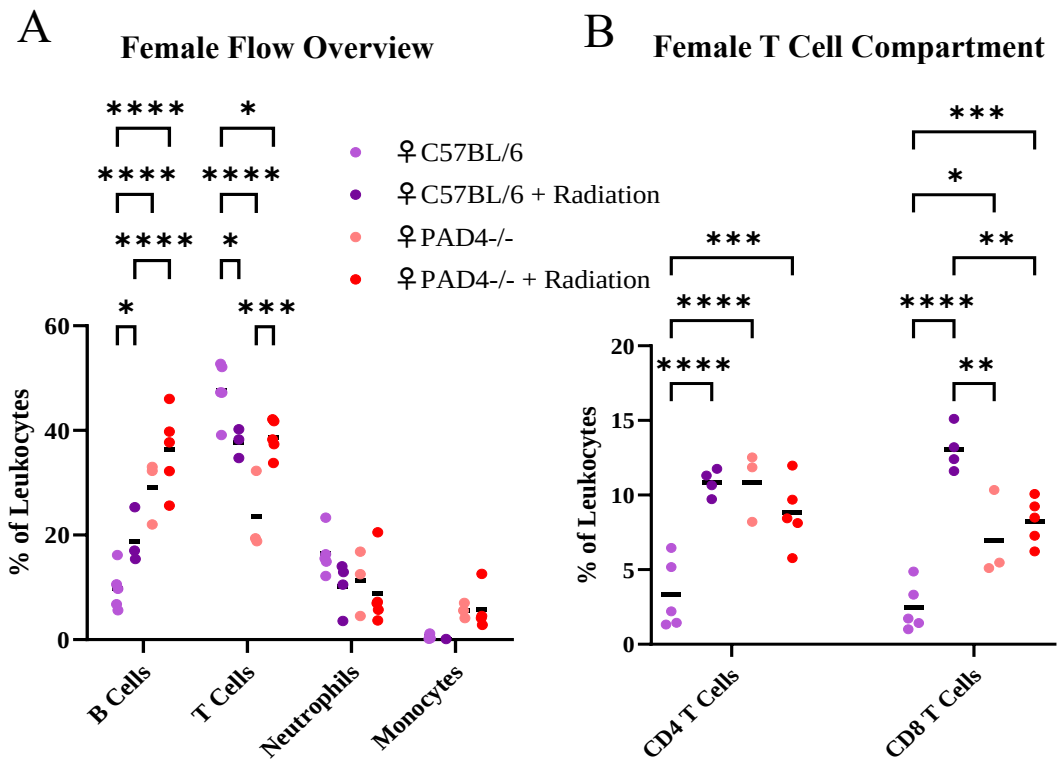

Fig 6: **A**, Overview of flow cytometry derived B Cell, T Cell, Neutrophil, and Monocyte abundance in the 4 female treatment groups. **B**, Overview of T Cell compartment in the 4 female treatment groups.

Section 10.07 Figure 7: Male Flow Cytometry Characterization

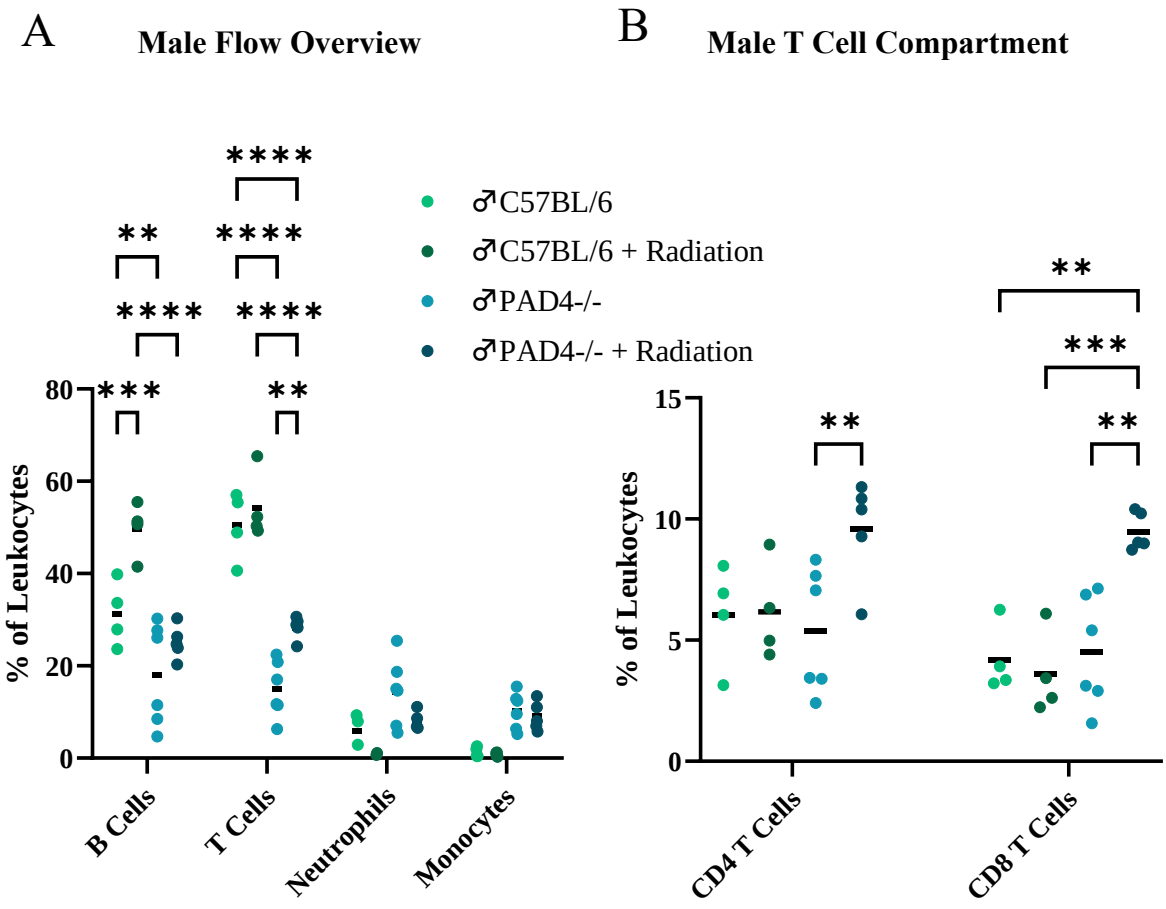

Fig 7: **A**, Overview of flow cytometry derived B Cell, T Cell, Neutrophil, and Monocyte abundance in the 4 male treatment groups. **B**, Overview of T Cell compartment in the 4 male treatment groups.

Section 10.08 Figure 8: Trial Workflow Schematic

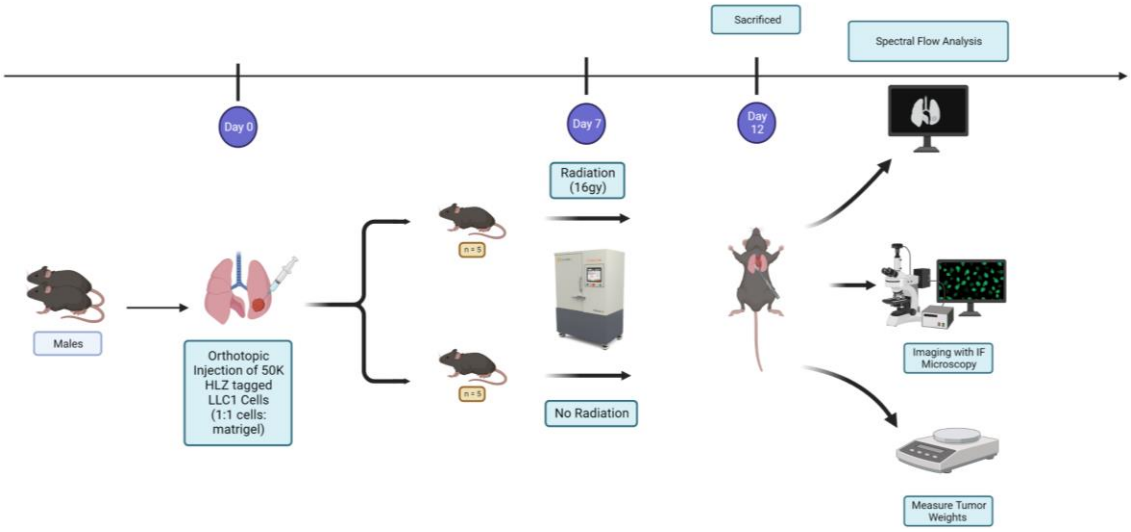

Fig 8: Schematic depicting trial workflow.

Section 10.09 Figure 9: Tumor Characteristics

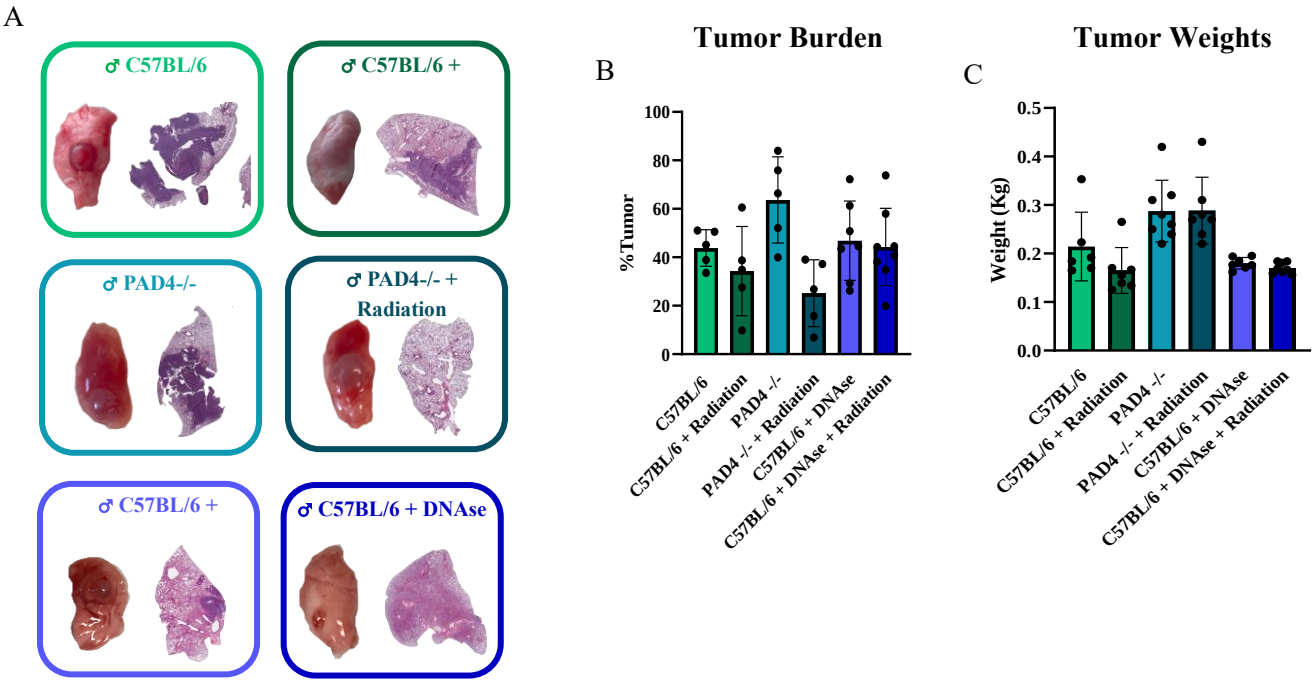

Fig 9: A, Tumor burden comparison between treatment groups including C57BL/6 (n=5), C57BL/6 + radiation, PAD4-/- (n=5), PAD4-/- + radiation, C57BL/6 + DNAse (n=5) and C57BL/6 + DNAse + radiation (n=5). **B**, Tumor weight comparison between treatment groups. **C**, Outline of 6 treatment groups. Representative lung images and histological H&E scans at end point for each treatment group.

Section 10.10 Figure 10: Tumor Microenvironment Halo Analysis

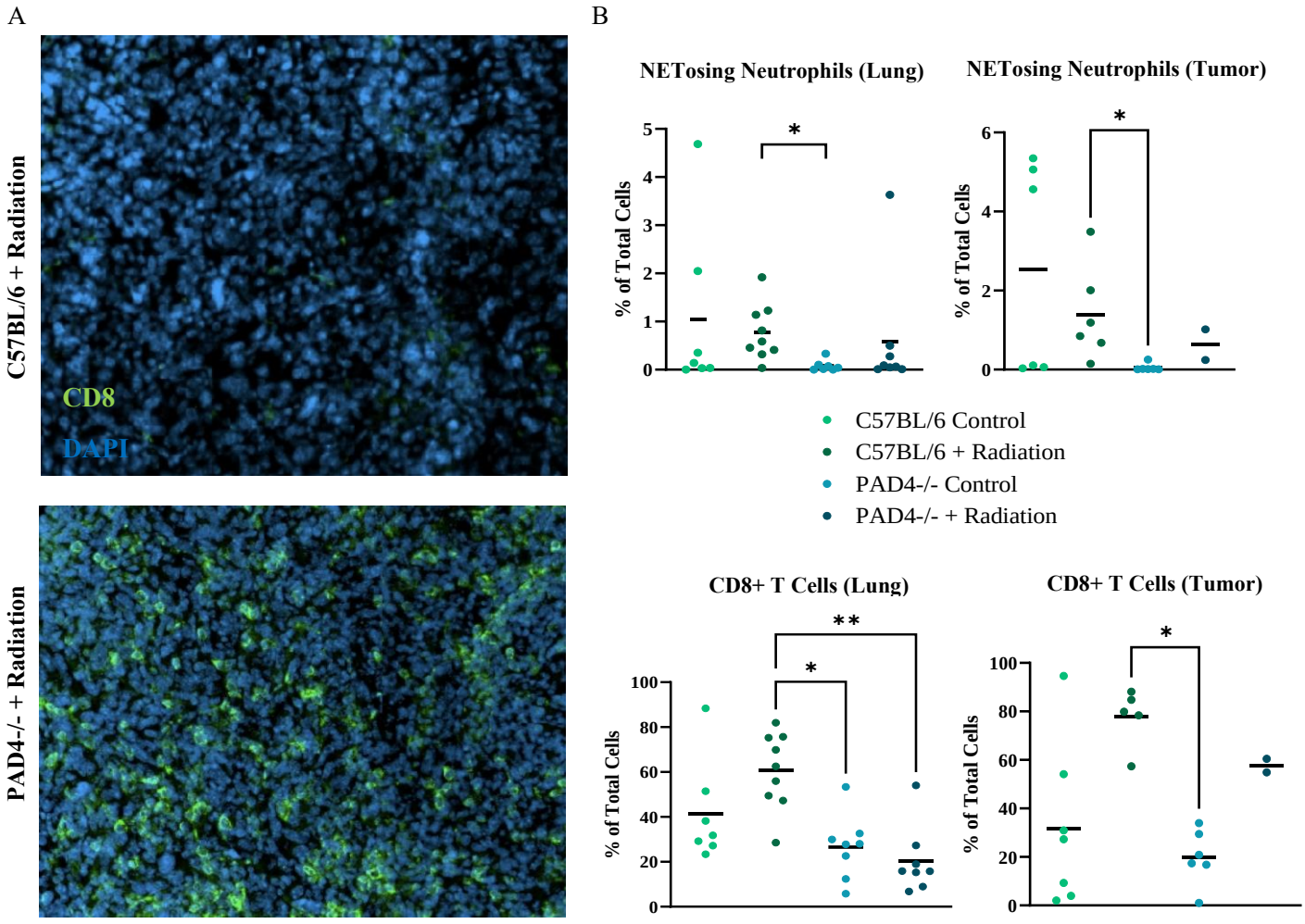

Fig 10: A, Representative immunofluorescence stain of CD8 in C57BL/6 irradiated vs. PAD4-/- irradiated tissue. **B**, Abundance of Netosing Neutrophils and CD8+ T cells in the lung and tumor beds.

Section 10.11 Figure 11: Leukocyte Compartment

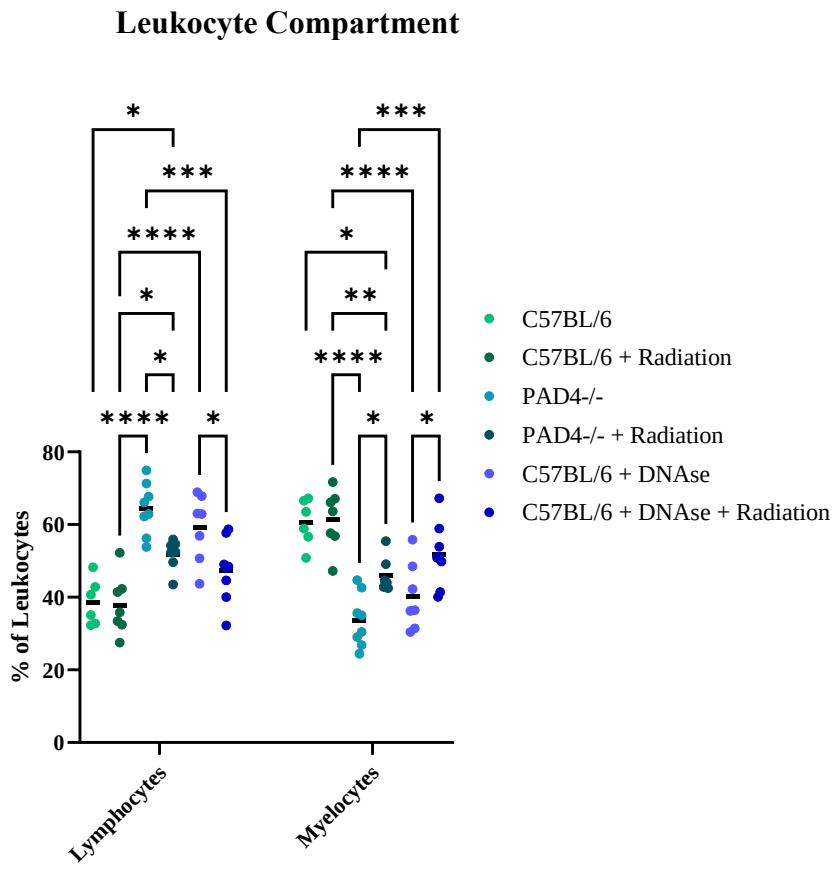

Fig 11: Distribution of lymphoid and myeloid niches from flow cytometry on treatment group lungs.

Section 10.12 Figure 12: Myeloid Compartment

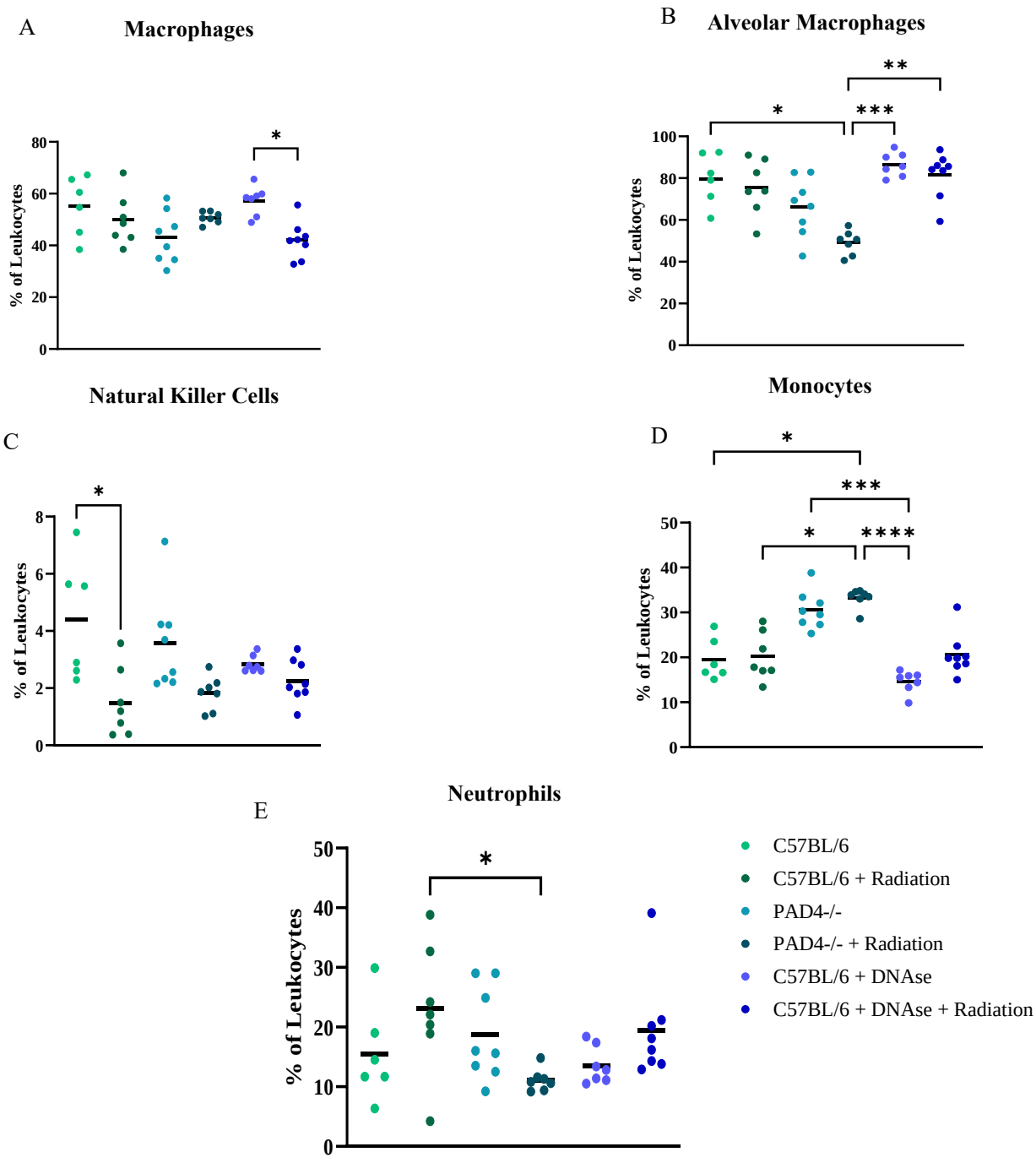

Fig 12: A, B, C, D, E, Flow cytometry from tumor bearing lungs depicting abundance of macrophages (**A**), alveolar macrophages (**B**), natural killer cells (**C**), monocytes (**D**), neutrophils (**E**).

Section 10.13 Figure 13: Lymphoid Compartment

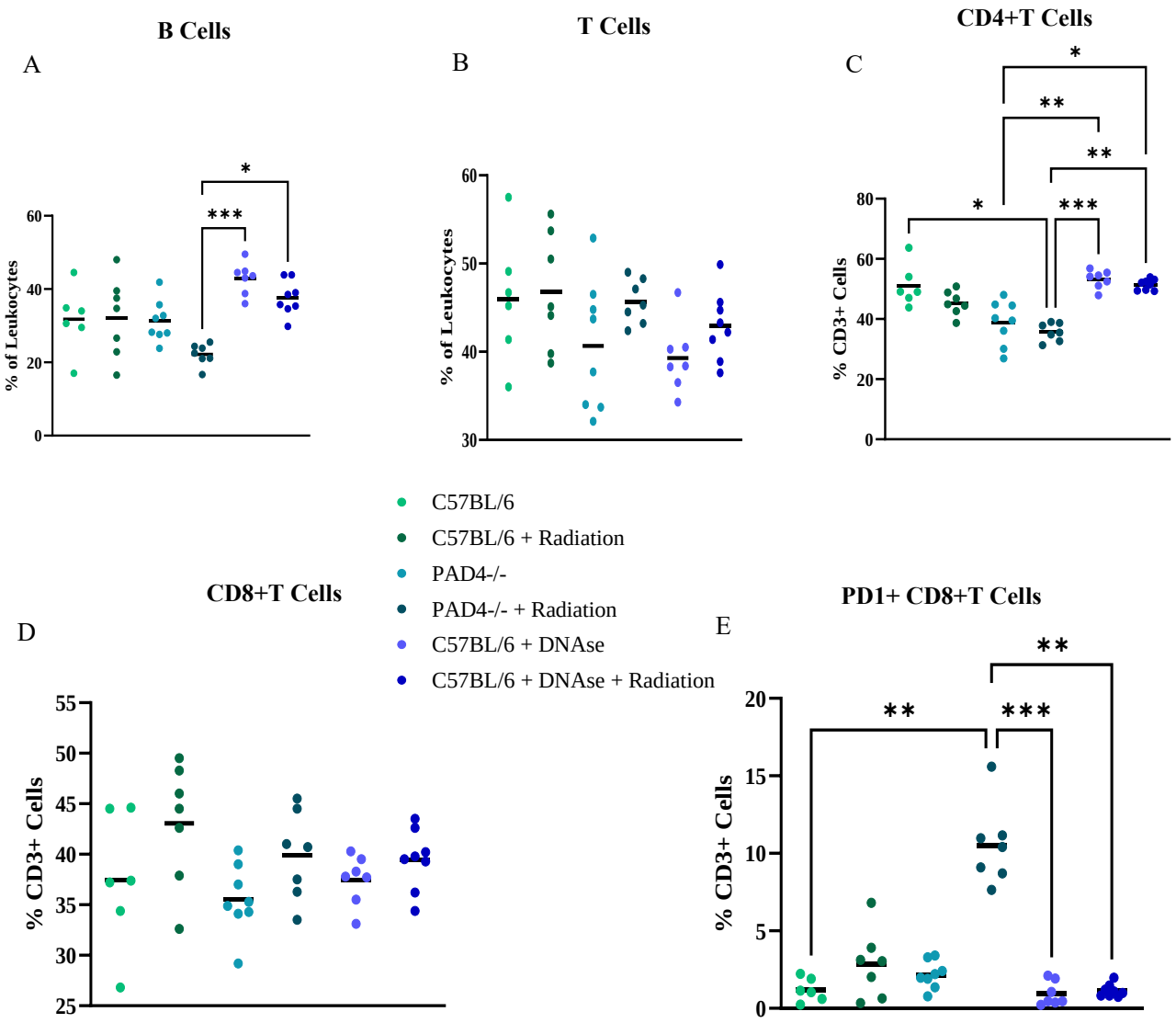

Fig 13: A, B, C, D, E, Flow cytometry from tumor bearing lungs depicting abundance of B cells (**A**), T Cells (**B**), CD4+ T Cells (**C**), CD8+ T Cells (**D**), PD1+ CD8 T Cells (**E**).

Section 10.14 Figure 14: Neutrophil to Lymphocyte Ratio

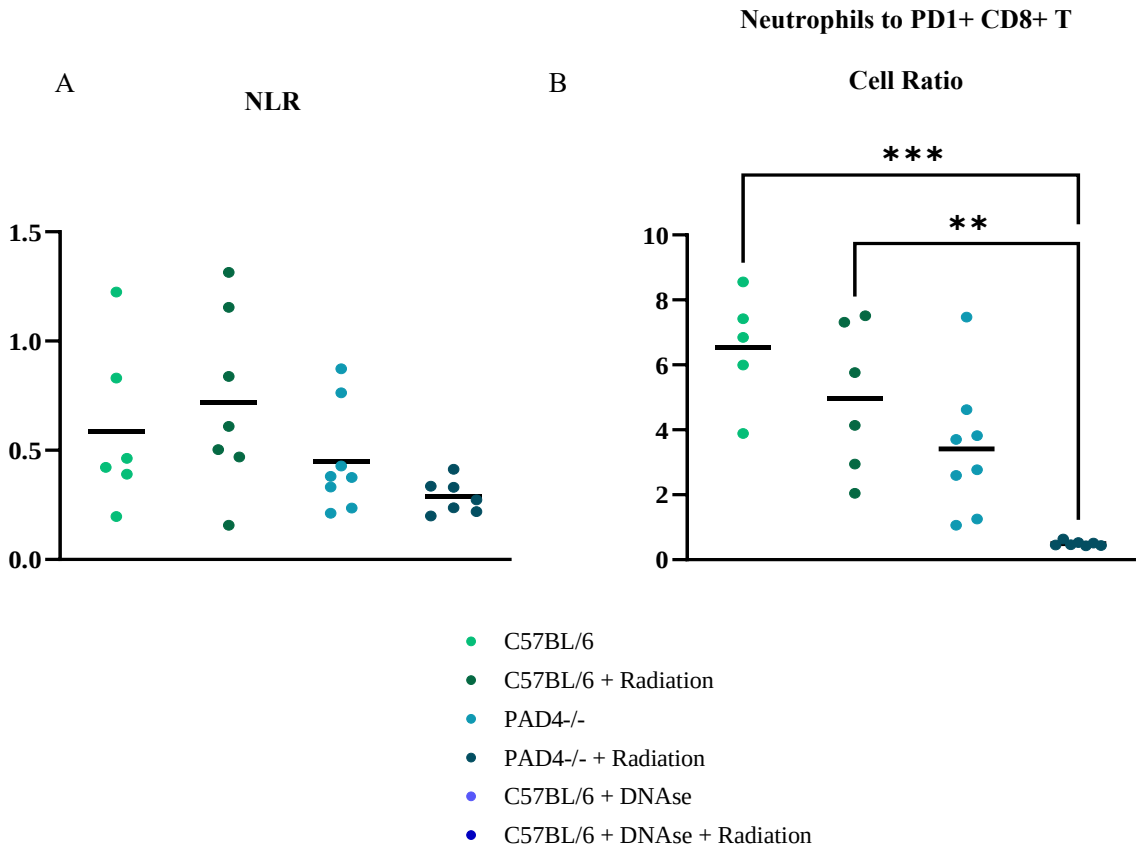

Fig 14: A, Neutrophil to lymphocyte ratio of each treatment group. **B**, Neutrophil to PD1+ CD8+ T cell ratio of each treatment group.

Section 10.15 Figure 15: Phenograph Heatmap

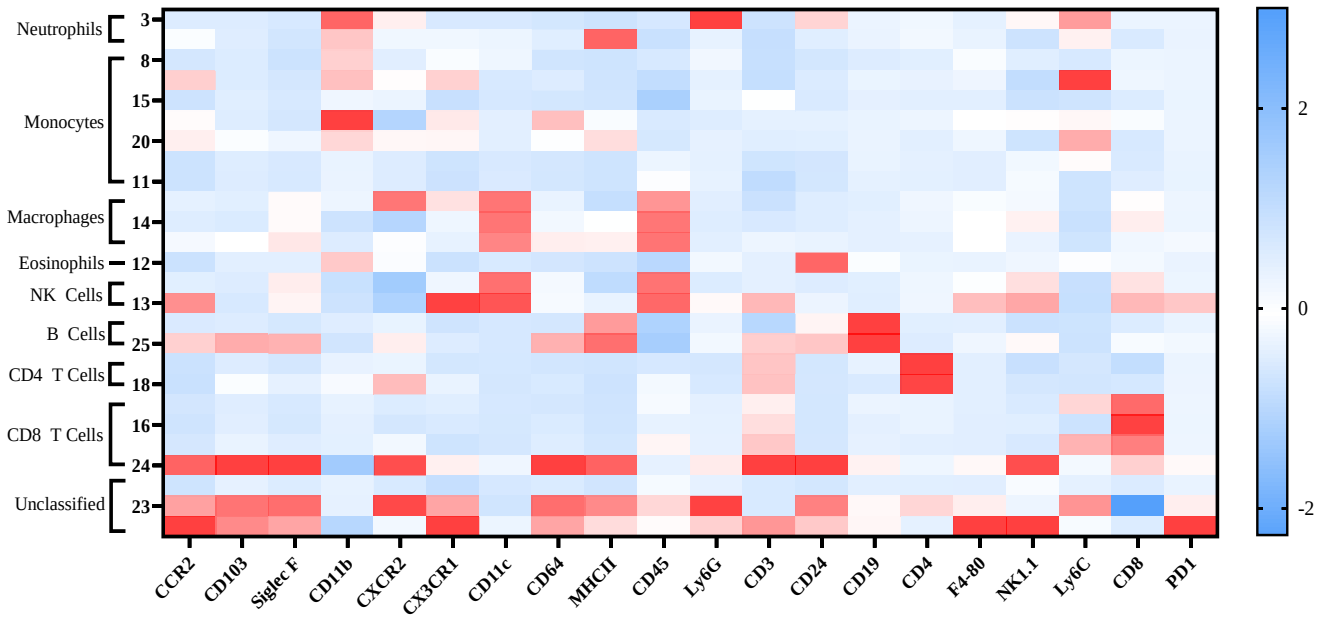

Fig 15: Heatmap representing PhenoGraph of unsupervised clustering of flow cytometry data classified by common immune cell types.

Section 10.16 Figure 16: Trial Workflow Schematic

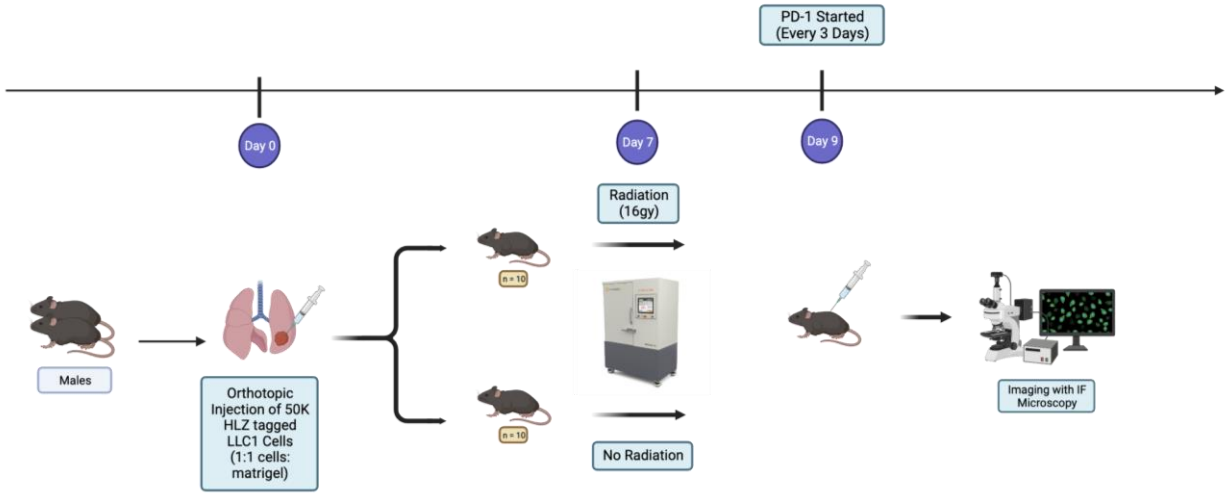

Fig 16: Schematic depicting ICI trial workflow.

Section 10.17 Figure 17: Survival Statistics

A B

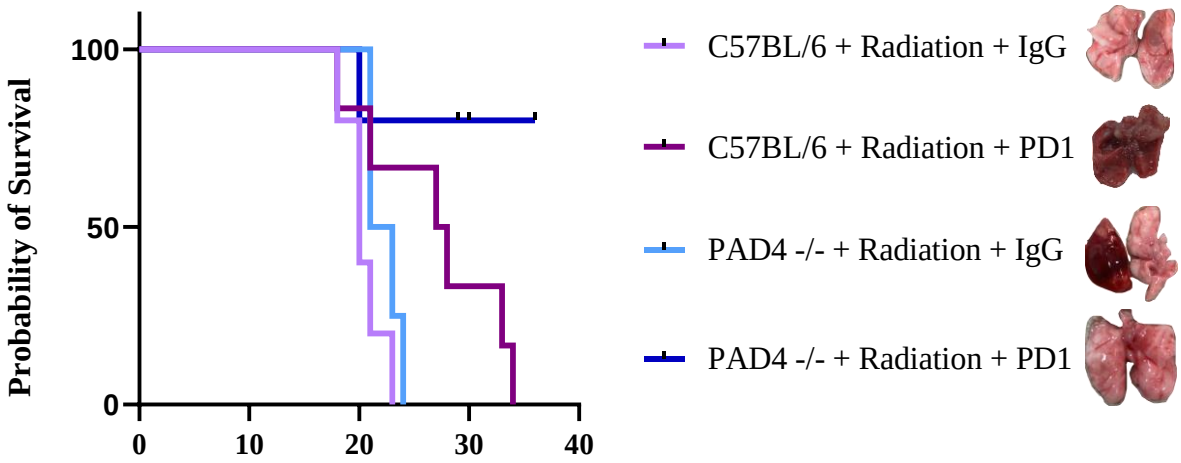

Fig 17: A, Kaplan Meier Survival plot of PAD4 -/- mice (n=10) vs C57BL/6 mice (n=10) after radiation and then treated with PD1 or vehicle IgG intraperitoneal injections. **B**, Lung images at endpoint of each treatment group.

Article XI. Discussion

Pad4 inhibition seemingly had a large effect on both tumor progression and severity. In *Pad4-/-* mice we saw massive changes in the lymphoid compartment characterized by general elevations in T cells. However, there were several elements of the first mouse trial that raises more questions about the applicability and mechanisms of *Pad4* inhibition. Firstly, *Pad4* inhibition alone did not confer longer survival in either sex. At day 17 and 22 for male and female mice respectively, mice appeared to reach endpoint, however, it is important to recognize that at this time *Pad4* KO mice had proportionally less tumor. Further, there was different tumor kinetics for each sex. Sex differences in cancer progression is a well characterized pan cancer phenotype with male cancers shown to be more aggressive in various cancers including glioblastomas [71,72]. Interestingly, one of the proposed mechanisms of cancer sex differences includes the deposition of intratumoral antigen experienced Tcf7/TCF1+ progenitor exhausted CD8+ T cells that lack effector activity due to intrinsic androgen receptor (AR) function [73]. While there are not stark differences in T cell abundance between sexes, we lack the necessary resolution to examine this compartment to properly elucidate what specific T cells populations are present in each sex. Further, there is also evidence to suggest that the regulation of *Pad4* expression is sex driven. Dong and colleagues demonstrate that *Pad4* expression can be driven by estrogen through the binding of estrogen receptor alpha to upstream of the *Pad4* gene and estrogen receptor alpha mediated enhancements of several activator proteins (AP) and nuclear factors (NF) including AP-1, AP-Sp1 and NF-Y [74]. This has several implications for this study as we noticed significant differences in tumor progression and the immune profiles between male and female mice. Interestingly, estrogen mediated *Pad4* expression would suggest an elevation in the capacity for NETosis in female mice in comparison to males. We would traditionally associate this observation with an aggressive

cancer phenotype in females, however, our work shows that females live longer than males with little changes in tumor burden at endpoint. A possibility here is that as research has shown, NETs are duplicitous in nature [11]. It is possible that while in male mice there are sufficient NETs to create a tumor faciliatory environment, promoting expansion and extraversion, in female mice NET deposition crosses a functional threshold – instead limiting cancer growth by encasing the tumor [61,63]. In this case we would expect to see a large increase in NETs via immunofluorescence analysis of female C57BL/6 tumors in comparison to male mice and is a necessary follow up experiment to confirm this relationship. However, estrogen driven *Pad4* expression would not explain differential sex survival in *Pad4-/-* mice. Unfortunately, we do not characterize the survival of these mice but elucidating whether sex-linked survival difference also exist in *Pad4-/-* mice would be a logical next step.

Moving on, we see similar phenotypes regarding tumor burden in C57BL/6 vs. *Pad4-/-* mice recapitulated at an earlier 12-day timepoint. However, flow cytometry and immunofluorescence data are not consistent in regards to the elevated PD1+ CD8 T cells we see via flow in irradiated *Pad4-/-* mice. While grossly, it appears that there is increased CD8+ T cell abundance in the tumor bed in irradiated *Pad4-/-* mice, HALO analysis shows that C57BL/6 mice on average had more CD8+ T Cell infiltration. There are several well characterized explanations for this phenotype. Firstly, we don't see tremendous changes in CD8+ T cell abundance between irradiated C57BL/6 and *Pad4-/-* groups suggesting that the inconsistencies in immunofluorescence data may be attributed to an absence of PD1 and CD8 co-staining. Elucidating whether HALO analysis of PD1+ CD8+ T cells corroborates the flow cytometry would be a natural follow up experiment. Additionally, in most of the *Pad4-/-* irradiated lungs there was little apparent tumor. This suggests that the immune response may have resolved itself leading to an efflux of many

important innate and adaptive immune cells. As a result, we would expect to see the CD8+ T cells that remain make up a larger proportion of the leukocyte compartment while still being less abundant than the T cells present in irradiated C57BL/6 mice.

It is also unclear what the identity is of the T cells that we see upregulated in irradiated *Pad4-/-* mice. Canonical markers of T cell exhaustion include $PD1^+$, $Lag3^+$, $Tim3^+$ and $TCF1^-$ [75-77]. In addition, exhausted $PD1^+$ T cells have been shown to respond extremely well to PD1 checkpoint blockade ameliorating cancer cell mediated T cell inhibition [78]. This is consistent with our observations regarding the response of irradiated *Pad4-/-* to subsequent PD1 checkpoint blockade. However, it also true that PD1 is expressed in tissue resident memory T cells (TRM) [79]. Further, in gastric cancer, $CD103^+$ $PD1^+$ TRMs have been shown to have better responses to immune checkpoint blockade [80]. The presence of a residual tissue resident memory T cell population would be consistent with our data showing a residual population of T cells in the lungs after immune resolution in irradiated *Pad4-/-* mice. If these cells are truly TRMs our data would suggest that NET inhibition enabled greater proliferation of resident T cells.

In the context of DNase 1 treatment, it did not appear that NET breakdown through this mechanism resulted in the same phenotype as *Pad4* knockout. DNase treated mice had comparable tumor burden to C57BL/6 treatment naïve mice and in terms of the immune landscape DNase treated mice were extremely inconsistent. Some myeloid populations represented C57BL/6 distributions while some of the lymphoid changes were similar to *Pad4-/-* mice in the corresponding conditions. This data is not completely unexpected as similar dynamics were observed in bladder cancer [10]. Work from the Spicer and Quail lab may provide a potential explanation. PhD candidate Simon Millette has demonstrated that neutrophils and NETs exhibit circadian cycling in circulation and in peripheral tissues. Since DNase 1 is short lived molecule,

the dissimilarity to *Pad4-/-* models may be due to pharmacokinetics and therapeutic administration could be better optimized to target NETs when they are most abundant. Another potential explanation is that functional NET inhibition may require more than physical denaturing of NETs DNA backbone structure. There is a possibility that the plethora of antimicrobial factors and cytokines released during NETosis play a critical pro-tumorigenic role, and are stifled with the absence of *Pad4*, an upstream actor. In terms of response to subsequent PD1 checkpoint blockade it is important to address that in the *Pad4-/-* + Radiation + PD1 inhibitor cohort, 2 mice had to be sacrificed before endpoint due to issues determined to be not related to lung cancer including trouble eating and lack of mobility. This was confirmed after mice were sacrificed by the absence of tumors in the primary lung . Unfortunately, a small number of mice weakens the power of our described relationship. In the future replicating this study to increase the power of our conclusions is a priority.

Thus far, we have demonstrated that *Pad4* inhibition leads to slower tumor progression and severity as well as an increase in $PD1^{+}$ $CD8^{+}$ T cell infiltration in the TME in murine models. This supports works previous established in bladder cancer as well as our own subcutaneous preliminary work [10]. Further, we have established the synergy of a NET-directed intervention to improve the efficacy of adjuvant immune checkpoint blockade after SABR. Interestingly we were not able to recapitulate this phenotype through breakdown of NETs using DNase 1, lending support to two main hypotheses. Either the extruded microbial factors and cytokines may be the key pro-tumorigenic actors of NETs or pharmacokinetics of DNase 1 inhibition were not sufficient to abrogate the effects of radiation on the TME.

In terms of future directions, we are actively trying to understand if these same dynamics are apparent in human patients with early-stage NSCLC through the SABR-BRIDGE cohort. The

SABR-BRIDGE cohort is a group of early-stage NSCLC patients that presented to the clinic during the SARS-CoV2 pandemic. Due to inaccessibility of operating rooms and divestment of resources towards high priority patients, the SABR-BRIDGE cohort instead received neoadjuvant radiation before being offered surgical resection 3-6 months later [81]. As a result, we have initial tumor biopsies and post-radiation resection specimens from several patients. This provides the unique opportunity to explore the dynamics of pre- and post-radiation response on the TME in multiple tumors. In order to address this, we have begun to analyze 1mm tumor cores from patients' biopsies and resections with imaging mass cytometry (IMC). IMC allows us to characterize the tumor immune microenvironment with incredible resolution, incorporating both lineage and activation state markers [70,82]. Through IMC we can assign specific cell identities to the T cell niche in order to corroborate our preclinical findings. Further, we are able to look at not only the cell-to-cell interactions – that is to say hypothetically seeing if the spatial proximity of T cells and macrophages confers better response to radiotherapy, but also entire cellular neighborhood interactions. Through cellular neighborhoods we can capture what spatial organizations of tumor cells, effector lymphoid cells, myeloid cells, and extra-cellular matrix (ECM) components like NETs are conducive for response or radio-resistance. Moreover, while our IMC panel traditionally uses over 40 markers to characterize the TME, it can be further optimized to reduce the number of markers needed to predict clinically meaningful outcomes. As a result, the clinical applicability of these potential findings is multifaceted. Firstly, if biopsies can be used to predict radiation response, clinicians will more readily be able to prescribe non-invasive treatment to patients that would benefit the most. Furthermore, in patients that have a TME that predicts radio resistance, the use of a *PAD4* small molecule inhibitor as an NET-directed intervention before SABR may

increase the effect of curative radiation as well as prime the TME for consolidation immunotherapy if necessary [83].

Overall, if similar mechanisms of radio-resistance are present in both mice and humans our data present a novel therapeutic approach to improving early stage radiation treatment in NSCLC as well as well as setting the foundation for prognostic clinical tests to streamline treatment and patient care. The SARS-CoV2 pandemic demonstrated the need to have strategies to increase the capacity that health care systems can provide to cancer patients even during times of extreme duress. Radiation treatment when optimized to be effective in more patients presents a robust, non-invasive therapeutic approach that reduces hospital visits, and resources while still providing curative potential in a cohort of patients that unless treated are among the worse in mortality at late-stage disease.

Article XII. Conclusion

Non-small cell lung cancer is the leading cause of cancer related mortality in Canada with 1 in 15 Canadians being diagnosed in their lifetimes [1]. Early-stage NSCLC patients makes up 30% of cases and the current standard of care includes lobectomy with radiotherapy primarily being used in patients that are inoperable or opt out of surgery. While limited by moderate rates of recurrence, radiation is a less invasive therapeutic approach that potentially could be leveraged to improve patient outcomes without perioperative risks. One of the key actors in radio-resistance are neutrophils extracellular traps (NETs) released from neutrophils in context of inflammation due to cancer and/or radiation. Here we sought to understand the role of NETs in radio-resistance in the unique microenvironment of the lung through preclinical models of NSCLC. We demonstrate that *Pad4*, an important enzyme in the NETosis pathway modulates response to radiation therapy.

Pad4-/- mice had decreased tumor burden and greater immune infiltrate in response to radiation as compared to wild-type mice. Interestingly, we find stark differences in both survival and immune dynamics between sexes, with female mice living longer with less CD8+ T Cell infiltration in comparison to male mice. In male mice, we leveraged this increased PD1+ CD8+ T cell infiltrate to improve the efficacy of adjuvant immune checkpoint blockade, establishing the therapeutic potential of a NET-driven intervention in this context. Next steps include the characterization of the SABR-BRIDGE cohort in order to elucidate if these same immune relationships exist in human patients. Improving radiation effectiveness presents a promising avenue of making early-stage treatment more accessible and effective, preventing the need to tackle NSCLC at later stages where mortality is far higher, and treatment associated toxicities much worse.

Article XIII. Bibliography

1 Society, C. C. Canadian Cancer Statistics: A 2022 Special Report on Cancer Prevelance. (2022).

2 Cancer, I. A. f. R. o. Global Cancer Observatory: Cancer Today. (2023).

3 Farjah, F., Flum, D. R., Varghese, T. K., Jr., Symons, R. G. & Wood, D. E. Surgeon specialty and long-term survival after pulmonary resection for lung cancer. *Ann Thorac Surg* **87**, 995-1004; discussion 1005-1006 (2009). https://doi.org:10.1016/j.athoracsur.2008.12.030

4 Videtic, G. M. M. *et al.* Stereotactic body radiation therapy for early-stage non-small cell lung cancer: Executive Summary of an ASTRO Evidence-Based Guideline. *Practical Radiation Oncology* **7**, 295-301 (2017). https://doi.org:10.1016/j.prro.2017.04.014

5 Tandberg, D. J., Tong, B. C., Ackerson, B. G. & Kelsey, C. R. Surgery versus stereotactic body radiation therapy for stage I non-small cell lung cancer: A comprehensive review. *Cancer* **124**, 667-678 (2018). https://doi.org:10.1002/cncr.31196

6 Fernández, C. *et al.* Single-fraction stereotactic ablative body radiation therapy for primary and metastasic lung tumor: A new paradigm? *World J Clin Oncol* **13**, 101-115 (2022). https://doi.org:10.5306/wjco.v13.i2.101

7 Sørensen, O. E. & Borregaard, N. Neutrophil extracellular traps — the dark side of neutrophils. *Journal of Clinical Investigation* **126**, 1612-1620 (2016). https://doi.org:10.1172/jci84538

8 Brinkmann, V. *et al.* Neutrophil extracellular traps kill bacteria. *Science* **303**, 1532-1535 (2004). https://doi.org:10.1126/science.1092385

9 Kaltenmeier, C. *et al.* Neutrophil Extracellular Traps Promote T Cell Exhaustion in the Tumor Microenvironment. *Frontiers in Immunology* **12** (2021). https://doi.org:10.3389/fimmu.2021.785222

10 Shinde-Jadhav, S. *et al.* Role of neutrophil extracellular traps in radiation resistance of invasive bladder cancer. *Nature Communications* **12** (2021). https://doi.org:10.1038/s41467-021-23086-z

11 Cools-Lartigue, J. *et al.* Neutrophil extracellular traps sequester circulating tumor cells and promote metastasis. *Journal of Clinical Investigation* **123**, 3446-3458 (2013). https://doi.org:10.1172/jci67484

12 Gridelli, C. *et al.* Non-small-cell lung cancer (Primer). *Nature Reviews: Disease Primers* **1** (2015). https://doi.org:https://doi.org/10.1038/nrdp.2015.9

13 Nicholson, A. G. *et al.* The 2021 WHO Classification of Lung Tumors: Impact of Advances Since 2015. *Journal of Thoracic Oncology* **17**, 362-387 (2022). https://doi.org:10.1016/j.jtho.2021.11.003

14 Travis, W. D., Brambilla, E. & Riely, G. J. New Pathologic Classification of Lung Cancer: Relevance for Clinical Practice and Clinical Trials. *Journal of Clinical Oncology* **31**, 992-1001 (2013). https://doi.org:10.1200/jco.2012.46.9270

15 Lababede, O. & Meziane, M. A. The Eighth Edition of TNM Staging of Lung Cancer: Reference Chart and Diagrams. *The Oncologist* **23**, 844-848 (2018). https://doi.org:10.1634/theoncologist.2017-0659

16 Hsin Feng, S. & Yang, S.-T. The new 8th TNM staging system of lung cancer and its potential imaging interpretation pitfalls and limitations with CT image demonstrations.

Diagnostic and Interventional Radiology **25**, 270-279 (2019). https://doi.org:10.5152/dir.2019.18458

17 Siegel, R. L., Miller, K. D., Fuchs, H. E. & Jemal, A. Cancer Statistics, 2021. *CA: A Cancer Journal for Clinicians* **71**, 7-33 (2021). https://doi.org:10.3322/caac.21654

18 Midthun, D. E. Early detection of lung cancer. *F1000Research* **5**, 739 (2016). https://doi.org:10.12688/f1000research.7313.1

19 Brawley, O. W. & Flenaugh, E. L. Low-dose spiral CT screening and evaluation of the solitary pulmonary nodule. *Oncology (Williston Park)* **28**, 441-446 (2014).

20 Reduced Lung-Cancer Mortality with Low-Dose Computed Tomographic Screening. *New England Journal of Medicine* **365**, 395-409 (2011). https://doi.org:10.1056/nejmoa1102873

21 Screening for Lung Cancer: U.S. Preventive Services Task Force Recommendation Statement. *Annals of Internal Medicine* **160**, 330-338 (2014). https://doi.org:10.7326/m13-2771 %m 24378917

22 Pastorino, U. *et al.* Annual or biennial CT screening versus observation in heavy smokers: 5-year results of the MILD trial. *Eur J Cancer Prev* **21**, 308-315 (2012). https://doi.org:10.1097/CEJ.0b013e328351e1b6

23 Infante, M. *et al.* Long-Term Follow-up Results of the DANTE Trial, a Randomized Study of Lung Cancer Screening with Spiral Computed Tomography. *American Journal of Respiratory and Critical Care Medicine* **191**, 1166-1175 (2015). https://doi.org:10.1164/rccm.201408-1475OC

24 Marmor, H. N., Zorn, J. T., Deppen, S. A., Massion, P. P. & Grogan, E. L. Biomarkers in lung cancer screening: a narrative review. *Current Challenges in Thoracic Surgery* **5**, 5-5 (2023). https://doi.org:10.21037/ccts-20-171

25 Pass, H. I., Beer, D. G., Joseph, S. & Massion, P. Biomarkers and molecular testing for early detection, diagnosis, and therapeutic prediction of lung cancer. *Thorac Surg Clin* **23**, 211-224 (2013). https://doi.org:10.1016/j.thorsurg.2013.01.002

26 Hassanein, M. *et al.* The state of molecular biomarkers for the early detection of lung cancer. *Cancer Prev Res (Phila)* **5**, 992-1006 (2012). https://doi.org:10.1158/1940-6207.Capr-11-0441

27 Howington, J. A., Blum, M. G., Chang, A. C., Balekian, A. A. & Murthy, S. C. Treatment of Stage I and II Non-small Cell Lung Cancer. *Chest* **143**, e278S-e313S (2013). https://doi.org:10.1378/chest.12-2359

28 Ginsberg, R. J. & Rubinstein, L. V. Randomized trial of lobectomy versus limited resection for T1 N0 non-small cell lung cancer. Lung Cancer Study Group. *Ann Thorac Surg* **60**, 615-622; discussion 622-613 (1995). https://doi.org:10.1016/0003-4975(95)00537-u

29 Donington, J., Schumacher, L. & Yanagawa, J. Surgical Issues for Operable Early-Stage Non–Small-Cell Lung Cancer. *Journal of Clinical Oncology* **40**, 530-538 (2022). https://doi.org:10.1200/jco.21.01592

30 Chaft, J. E. *et al.* Evolution of systemic therapy for stages I–III non-metastatic non-small-cell lung cancer. *Nature Reviews Clinical Oncology* **18**, 547-557 (2021). https://doi.org:10.1038/s41571-021-00501-4

31 Saji, H. *et al.* Segmentectomy versus lobectomy in small-sized peripheral non-small-cell lung cancer (JCOG0802/WJOG4607L): a multicentre, open-label, phase 3, randomised, controlled, non-inferiority trial. *The Lancet* **399**, 1607-1617 (2022). https://doi.org:https://doi.org/10.1016/S0140-6736(21)02333-3

32 Altorki, N. *et al.* Lobar or Sublobar Resection for Peripheral Stage IA Non–Small-Cell Lung Cancer. *New England Journal of Medicine* **388**, 489-498 (2023). https://doi.org:10.1056/nejmoa2212083

33 Chen, H. *et al.* Stereotactic Ablative Radiation Therapy Versus Surgery in Early Lung Cancer: A Meta-analysis of Propensity Score Studies. *International Journal of Radiation Oncology*Biology*Physics* **101**, 186-194 (2018). https://doi.org:https://doi.org/10.1016/j.ijrobp.2018.01.064

34 Berzenji, L. & Van Schil, P. E. Surgery or stereotactic body radiotherapy for early-stage lung cancer: two sides of the same coin? *European Respiratory Journal* **53**, 1900711 (2019). https://doi.org:10.1183/13993003.00711-2019

35 Maquilan, G. & Timmerman, R. Stereotactic Body Radiation Therapy for Early-Stage Lung Cancer. *Cancer J* **22**, 274-279 (2016). https://doi.org:10.1097/ppo.0000000000000204

36 Chang, J. Y. *et al.* Stereotactic ablative radiotherapy with or without immunotherapy for early-stage or isolated lung parenchymal recurrent node-negative non-small-cell lung cancer: an open-label, randomised, phase 2 trial. *The Lancet* **402**, 871-881 (2023). https://doi.org:https://doi.org/10.1016/S0140-6736(23)01384-3

37 White, A. & Swanson, S. J. Minimally Invasive Surgery for Early-Stage Lung Cancer: From Innovation to Standard of Care. *Oncology (Williston Park)* **30**, 982-987 (2016).

38 Arriagada, R. *et al.* Adjuvant chemotherapy, with or without postoperative radiotherapy, in operable non-small-cell lung cancer: two meta-analyses of individual patient data. *Lancet* **375**, 1267-1277 (2010). https://doi.org:10.1016/s0140-6736(10)60059-1

39 Antonia, S. J. *et al.* Overall Survival with Durvalumab after Chemoradiotherapy in Stage III NSCLC. *New England Journal of Medicine* **379**, 2342-2350 (2018). https://doi.org:10.1056/nejmoa1809697

40 Gilligan, D. *et al.* Preoperative chemotherapy in patients with resectable non-small cell lung cancer: results of the MRC LU22/NVALT 2/EORTC 08012 multicentre randomised trial and update of systematic review. *The Lancet* **369**, 1929-1937 (2007). https://doi.org:https://doi.org/10.1016/S0140-6736(07)60714-4

41 Chen, X. & Ma, K. Neoadjuvant Therapy in Lung Cancer: What Is Most Important: Objective Response Rate or Major Pathological Response? *Current Oncology* **28**, 4129-4138 (2021). https://doi.org:10.3390/curroncol28050350

42 Forde, P. M. *et al.* Neoadjuvant Nivolumab plus Chemotherapy in Resectable Lung Cancer. *New England Journal of Medicine* **386**, 1973-1985 (2022). https://doi.org:10.1056/nejmoa2202170

43 Cascone, T. *et al.* Checkmate 77T: A phase III trial of neoadjuvant nivolumab (NIVO) plus chemotherapy (chemo) followed by adjuvant nivo in resectable early-stage NSCLC. *Journal of Clinical Oncology* **38**, TPS9076-TPS9076 (2020). https://doi.org:10.1200/JCO.2020.38.15_suppl.TPS9076

44 Wakelee, H. A. *et al.* KEYNOTE-671: Randomized, double-blind, phase 3 study of pembrolizumab or placebo plus platinum-based chemotherapy followed by resection and

pembrolizumab or placebo for early stage NSCLC. *Journal of Clinical Oncology* **41**, LBA100-LBA100 (2023). https://doi.org:10.1200/jco.2023.41.17_suppl.lba100

45 Lu, S. *et al.* Perioperative toripalimab + platinum-doublet chemotherapy vs chemotherapy in resectable stage II/III non-small cell lung cancer (NSCLC): Interim event-free survival (EFS) analysis of the phase III Neotorch study. *Journal of Clinical Oncology* **41**, 425126-425126 (2023). https://doi.org:10.1200/jco.2023.41.36_suppl.425126

46 Haager, B. *et al.* AEGEAN: A phase 3 trial of neoadjuvant durvalumab+chemotherapy followed by adjuvant durvalumab in patients with resectable NSCLC. *Zentralbl Chir* **148**, P-228 (2023). https://doi.org:10.1055/s-0043-1771092

47 Wu, Y.-L. *et al.* Osimertinib in ResectedEGFR-Mutated Non–Small-Cell Lung Cancer. *New England Journal of Medicine* **383**, 1711-1723 (2020). https://doi.org:10.1056/nejmoa2027071

48 Solomon, B. J. *et al.* ALINA: A phase III study of alectinib versus chemotherapy as adjuvant therapy in patients with stage IB–IIIA anaplastic lymphoma kinase-positive (ALK+) non-small cell lung cancer (NSCLC). *Journal of Clinical Oncology* **37**, TPS8569-TPS8569 (2019). https://doi.org:10.1200/JCO.2019.37.15_suppl.TPS8569

49 Hiley, C. T. *et al.* Challenges in molecular testing in non-small-cell lung cancer patients with advanced disease. *Lancet* **388**, 1002-1011 (2016). https://doi.org:10.1016/s0140-6736(16)31340-x

50 Coffelt, S. B., Wellenstein, M. D. & De Visser, K. E. Neutrophils in cancer: neutral no more. *Nature Reviews Cancer* **16**, 431-446 (2016). https://doi.org:10.1038/nrc.2016.52

51 Mayadas, T. N., Cullere, X. & Lowell, C. A. The Multifaceted Functions of Neutrophils. *Annual Review of Pathology: Mechanisms of Disease* **9**, 181-218 (2014). https://doi.org:10.1146/annurev-pathol-020712-164023

52 Nauseef, W. M. & Borregaard, N. Neutrophils at work. *Nature Immunology* **15**, 602-611 (2014). https://doi.org:10.1038/ni.2921

53 Amulic, B., Cazalet, C., Hayes, G. L., Metzler, K. D. & Zychlinsky, A. Neutrophil Function: From Mechanisms to Disease. *Annual Review of Immunology* **30**, 459-489 (2012). https://doi.org:10.1146/annurev-immunol-020711-074942

54 Liew, P. X. & Kubes, P. The Neutrophil's Role During Health and Disease. *Physiological Reviews* **99**, 1223-1248 (2019). https://doi.org:10.1152/physrev.00012.2018

55 Mishalian, I. *et al.* Tumor-associated neutrophils (TAN) develop pro-tumorigenic properties during tumor progression. *Cancer Immunology, Immunotherapy* **62**, 1745-1756 (2013). https://doi.org:10.1007/s00262-013-1476-9

56 Shaul, M. E. & Fridlender, Z. G. Neutrophils as active regulators of the immune system in the tumor microenvironment. *Journal of Leukocyte Biology* **102**, 343-349 (2017). https://doi.org:10.1189/jlb.5mr1216-508r

57 Castanheira, F. V. S. & Kubes, P. Neutrophils and NETs in modulating acute and chronic inflammation. *Blood* **133**, 2178-2185 (2019). https://doi.org:https://doi.org/10.1182/blood-2018-11-844530

58 Papayannopoulos, V., Metzler, K. D., Hakkim, A. & Zychlinsky, A. Neutrophil elastase and myeloperoxidase regulate the formation of neutrophil extracellular traps. *J Cell Biol* **191**, 677-691 (2010). https://doi.org:10.1083/jcb.201006052

59 Teijeira, Á. *et al.* CXCR1 and CXCR2 Chemokine Receptor Agonists Produced by Tumors Induce Neutrophil Extracellular Traps that Interfere with Immune Cytotoxicity. *Immunity* **52**, 856-871.e858 (2020). https://doi.org:10.1016/j.immuni.2020.03.001

60 Cedervall, J. *et al.* Neutrophil Extracellular Traps Accumulate in Peripheral Blood Vessels and Compromise Organ Function in Tumor-Bearing Animals. *Cancer Res* **75**, 2653-2662 (2015). https://doi.org:10.1158/0008-5472.Can-14-3299

61 Demers, M. & Wagner, D. D. Neutrophil extracellular traps. *OncoImmunology* **2**, e22946 (2013). https://doi.org:10.4161/onci.22946

62 Albrengues, J. *et al.* Neutrophil extracellular traps produced during inflammation awaken dormant cancer cells in mice. *Science* **361**, eaao4227 (2018). https://doi.org:10.1126/science.aao4227

63 Demers, M. *et al.* Cancers predispose neutrophils to release extracellular DNA traps that contribute to cancer-associated thrombosis. *Proceedings of the National Academy of Sciences* **109**, 13076-13081 (2012). https://doi.org:10.1073/pnas.1200419109

64 Mcdowell, S. A. C. *et al.* Neutrophil oxidative stress mediates obesity-associated vascular dysfunction and metastatic transmigration. *Nature Cancer* **2**, 545-562 (2021). https://doi.org:10.1038/s43018-021-00194-9

65 Kaltenmeier, C. *et al.* Time to Surgery and Colon Cancer Survival in the United States. *Ann Surg* **274**, 1025-1031 (2021). https://doi.org:10.1097/sla.0000000000003745

66 Masucci, M. T., Minopoli, M., Del Vecchio, S. & Carriero, M. V. The Emerging Role of Neutrophil Extracellular Traps (NETs) in Tumor Progression and Metastasis. *Front Immunol* **11**, 1749 (2020). https://doi.org:10.3389/fimmu.2020.01749

67 Wu, L., Saxena, S. & Singh, R. K. in *Advances in Experimental Medicine and Biology* 1-20 (Springer International Publishing, 2020).

68 Kaltenmeier, C. *et al.* Neutrophil Extracellular Traps Promote T Cell Exhaustion in the Tumor Microenvironment. *Front Immunol* **12**, 785222 (2021). https://doi.org:10.3389/fimmu.2021.785222

69 Wang, B., Su, X., Zhang, B. & Pan, S. GSK484, an inhibitor of peptidyl arginine deiminase 4, increases the radiosensitivity of colorectal cancer and inhibits neutrophil extracellular traps. *The Journal of Gene Medicine* **25** (2023). https://doi.org:10.1002/jgm.3530

70 Sorin, M. *et al.* Single-cell spatial landscapes of the lung tumour immune microenvironment. *Nature* **614**, 548-554 (2023). https://doi.org:10.1038/s41586-022-05672-3

71 Haupt, S., Caramia, F., Klein, S. L., Rubin, J. B. & Haupt, Y. Sex disparities matter in cancer development and therapy. *Nature Reviews Cancer* **21**, 393-407 (2021). https://doi.org:10.1038/s41568-021-00348-y

72 Yang, W. *et al.* Sex differences in GBM revealed by analysis of patient imaging, transcriptome, and survival data. *Science Translational Medicine* **11**, eaao5253 (2019). https://doi.org:10.1126/scitranslmed.aao5253

73 Kwon, H. *et al.* Androgen conspires with the CD8(+) T cell exhaustion program and contributes to sex bias in cancer. *Sci Immunol* **7**, eabq2630 (2022). https://doi.org:10.1126/sciimmunol.abq2630

74 Dong, S., Zhang, Z. & Takahara, H. Estrogen-Enhanced Peptidylarginine Deiminase Type IV Gene (PADI4) Expression in MCF-7 Cells Is Mediated by Estrogen Receptor-α-

Promoted Transfactors Activator Protein-1, Nuclear Factor-Y, and Sp1. *Molecular Endocrinology* **21**, 1617-1629 (2007). https://doi.org:10.1210/me.2006-0550

75 Blank, C. U. *et al.* Defining 'T cell exhaustion'. *Nature Reviews Immunology* **19**, 665-674 (2019). https://doi.org:10.1038/s41577-019-0221-9

76 Wherry, E. J. T cell exhaustion. *Nature Immunology* **12**, 492-499 (2011). https://doi.org:10.1038/ni.2035

77 Yi, J. S., Cox, M. A. & Zajac, A. J. T-cell exhaustion: characteristics, causes and conversion. *Immunology* **129**, 474-481 (2010). https://doi.org:10.1111/j.1365-2567.2010.03255.x

78 Alsaab, H. O. *et al.* PD-1 and PD-L1 Checkpoint Signaling Inhibition for Cancer Immunotherapy: Mechanism, Combinations, and Clinical Outcome. *Frontiers in Pharmacology* **8** (2017). https://doi.org:10.3389/fphar.2017.00561

79 Mami-Chouaib, F. & Tartour, E. Editorial: Tissue Resident Memory T Cells. *Frontiers in Immunology* **10** (2019). https://doi.org:10.3389/fimmu.2019.01018

80 Nose, Y. *et al.* The tissue-resident marker CD103 on peripheral blood T cells predicts responses to anti-PD-1 therapy in gastric cancer. *Cancer Immunology, Immunotherapy* **72**, 169-181 (2023). https://doi.org:10.1007/s00262-022-03240-2

81 Kidane, B. *et al.* SABR-BRIDGE: Stereotactic ABlative Radiotherapy Before Resection to AvoId Delay for Early-Stage LunG Cancer or OligomEts During the COVID-19 Pandemic. *Front Oncol* **10**, 580189 (2020). https://doi.org:10.3389/fonc.2020.580189

82 Karimi, E. *et al.* Single-cell spatial immune landscapes of primary and metastatic brain tumours. *Nature* **614**, 555-563 (2023). https://doi.org:10.1038/s41586-022-05680-3

83 Lewis, H. D. *et al.* Inhibition of PAD4 activity is sufficient to disrupt mouse and human NET formation. *Nature Chemical Biology* **11**, 189-191 (2015). https://doi.org:10.1038/nchembio.1735